

# LatentLLM: Attention-Aware Joint Tensor Compression

Toshiaki Koike-Akino, Xiangyu Chen, Jing Liu, Ye Wang, Pu (Perry) Wang, Matthew Brand

Mitsubishi Electric Research Laboratories (MERL), Cambridge, MA 02139, USA

{koike, xiachen, jiliu, yewang, pwang, brand}@merl.com

## Abstract

*Modern foundation models such as large language models (LLMs) and large multi-modal models (LMMs) require a massive amount of computational and memory resources. We propose a new framework to convert such LLMs/LMMs into a reduced-dimension latent structure. Our method extends a local activation-aware tensor decomposition to a global attention-aware joint tensor decomposition. Our framework can significantly improve the model accuracy over the existing model compression methods when reducing the latent dimension to realize computationally/memory-efficient LLMs/LLMs. We show the benefit on several benchmark including multi-modal reasoning tasks.*

## 1. Introduction

Large language models (LLMs) [1, 39] and large multi-modal models (LMMs) [25] have shown excellent performance across a variety of general tasks [4, 16, 42]. Nonetheless, these models having billions of parameters demand significant computational resources [36]. Towards increasing the accessibility and sustainability of LLMs/LMMs, extensive efforts have been devoted to model compression [2, 44, 50]: e.g., partial activation [15, 22], pruning [3, 10, 12, 38], quantization [11, 23, 40], knowledge distillation [7, 13, 14], and low-rank factorization [14, 24, 34, 47].

More recently, the reduced-dimension LLM DeepSeek-V3 [24] has attracted much attention for its high efficiency and performance. It employs a low-rank architecture called multi-head latent attention (MLA) to compress the standard multi-head attention (MHA), realizing an efficient KV cache [5, 34], accelerated training, and high-performance inference. In this paper, we provide a novel solution to convert a pretrained LLM/LMM built with MHA into a compressed LLM/LMM with a type of MLA. Our approach is motivated by a global compression framework introduced in SparseLLM [3] and Q-VLM [40]. Although the original method was designed for pruning/quantization, we adopt

it for tensor rank reduction. We further extended it to the joint compression of MHA, while the original SparseLLM was for compressing the multi-layer perceptron (MLP) part. Our derived solution is based on a high-order tensor-rank decomposition to jointly factorize multiple linear layers.

The contributions of our paper are summarized below.

- We propose a novel low-rank decomposition approach called LatentLLM to compress LLMs/LMMs.
- We discuss an optimal pre-conditioning for activation-aware SVD.
- We reveal that a choice of junction matrix can significantly reduce the model size.
- We then introduce an attention-aware joint SVD framework to compress multiple weights at the same time.
- Our experiments validate that our LatentLLM approach can improve the performance of LLM/LMM compression over existing methods.
- The latent LLaVa with our method offers a significant advantage in multi-modal reasoning capability.

## 2. Related work

**Model compression** The field of model compression for LLMs/LMMs has seen a surge of innovative techniques aimed at mitigating the substantial computation and memory requirements [48, 50]. Various methods have emerged to address this challenge, each taking a unique approach to reduce the memory footprint of LLMs/LMMs. These methods primarily fall into four categories: weight quantization [11, 23, 40], network pruning [3, 10, 12, 18], knowledge distillation [7, 13, 14], and low-rank factorization [14, 24, 32, 34, 47].

Among these methods, weight quantization has gained significant traction in the context of large foundation models due to its effectiveness. However, all four compression techniques are orthogonal and can be applied together. Recognizing this, we introduce a novel low-rank decomposition method which jointly compresses multiple layers of an LLM/LMM in a training-free manner.

**Low-rank decomposition** In the realm of low-rank decomposition [35] for neural network compression, exist-

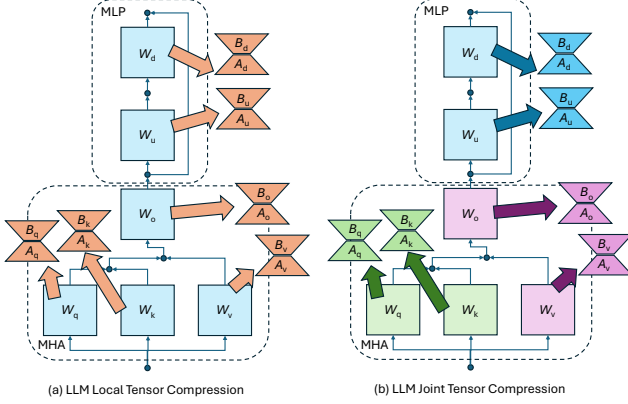


Figure 1. Reduced-dimension LLM/LMM with low-rank tensor decomposition. (a) each linear modules are locally compressed by activation-aware tensor decomposition. (b) multiple linear modules are globally compressed by attention-aware tensor decomposition.

ing methods typically involve decomposing weight matrices of pre-trained networks using techniques like Singular Value Decomposition (SVD) or tensor decomposition, followed by fine-tuning the factorized network [8, 33]. LoSparse [20] uses low-rank approximation plus a sparse matrix to compress the weight matrix in transformers. Similarly, CALDERA [32] uses low-rank approximation plus a quantized matrix. ASVD [47] significantly improves the low-rank decomposition by dealing with activation statistics. It was applied to SVD-LLM [41] and Palu [5]. DeepSeek-V3 [24] employs the similar latent reduction via MLA to make MHA efficient and capable. Eigen attention [34] is highly related to MLA.

### 3. LatentLLM: Tensor compression

#### 3.1. Reduced-dimension LLM/LMM

Fig. 1 illustrates the basic transformer architecture consisting of MHA and MLP, used in some LLMs/LMMs. For MLP, there are up and down projections, whereas MHA has query/key/value/output projections. By transforming those dense weight matrices into low-rank decompositions, we can realize an efficient latent LLM/LMM having potential benefits: (i) fewer-parameter model size; (ii) KV cache reduction; (iii) accelerated processing; (iv) lower-power consumption. In fact, some recent LLM models such as DeepSeek-V3 [24] demonstrated efficiency and high-performance with MLA. We focus on compressing a pre-trained LLM/LMM by converting MHA into a type of MLA in a zero-shot fashion, i.e., without any fine-tuning.

Most existing compression methods are based on a local loss minimization to approximate each weight individually. Motivated by recent work towards global optimization with

SparseLLM [3] and Q-VLM [40], we propose a joint tensor compression framework that we call “LatentLLM.” Specifically, we derive a mathematical solution to jointly decompose a pair of query and value projections, a pair of value and output projections, and a pair of up and down projections to compress LLMs/LMMs.

Before describing our solution, we first address activation-aware compression. We provide some new insights on the choice of pre-conditioner and junction matrix below.

#### 3.2. Activation-aware SVD: Pre-conditioning

A pioneering work by ASVD [47] introduced a way to compress a layer depending on the activation statistics. Consider a pretrained-weight  $W \in \mathbb{R}^{d' \times d}$  to compress with a lower-rank decomposition  $\hat{W} = BA$  for compression matrix  $A \in \mathbb{R}^{r \times d}$  and decompression matrix  $B \in \mathbb{R}^{d' \times r}$ . Using the input activation  $X \in \mathbb{R}^{d \times l}$  ( $l$  is the calibration sample length), ASVD aims to minimize the activation loss:

$$\mathcal{L}_1 = \mathbb{E}_X \|WX - \hat{W}X\|^2 = \mathbb{E}_X \|WX - BAX\|^2, \quad (1)$$

instead of the naïve weight-based loss:

$$\mathcal{L}_0 = \|W - \hat{W}\|^2 = \|W - BA\|^2. \quad (2)$$

It is well-known that the optimal solution to minimize  $\mathcal{L}_0$  can be given by the plain SVD of  $W$ . To minimize  $\mathcal{L}_1$ , ASVD introduced a pre-conditioning matrix  $P \in \mathbb{R}^{d \times d}$  to whiten the statistical impact of the activation  $X$ . Specifically, ASVD uses the low-rank matrices given by whitened SVD:

$$BAP = \text{svd}_r[WP], \quad (3)$$

where  $\text{svd}_r[\cdot]$  denotes the rank- $r$  truncated SVD.

Although ASVD originally suggested a diagonal  $\ell_1$ -norm pre-conditioning, the optimal pre-conditioning matrix  $P$  can be given by reformulating  $\mathcal{L}_1$  as follows:

$$\mathcal{L}_1 = \text{tr}[(W - BA)\mathbb{E}_X[XX^\top](W - BA)^\top] \quad (4)$$

$$= \|(W - BA)C^{\frac{1}{2}}\|^2 = \|WC^{\frac{1}{2}} - BAC^{\frac{1}{2}}\|^2, \quad (5)$$

where  $C = \mathbb{E}_X[XX^\top] \in \mathbb{R}^{d \times d}$  is a covariance (precisely, auto-correlation) of input activation. Hence, the above loss can be minimized by the SVD:  $BAC^{\frac{1}{2}} = \text{svd}_r[WC^{\frac{1}{2}}]$ . Accordingly, it is found that the optimal pre-conditioner is the square-root covariance:  $P = C^{\frac{1}{2}}$ . Given the finite calibration data  $X$ , we can estimate the covariance as  $C = XX^\top + \lambda I$ , where the damping factor  $\lambda \in \mathbb{R}_+$  corresponds to the shrunk estimator [19].

**Remark 1** Different pre-conditioning methods were introduced in several techniques including pruning and quantization, as listed in Tab. 1. As those variants are sub-optimal,

Table 1. Variants of pre-conditioning matrices  $P$  for activation-aware distillation.

Conditioning $P$	Expression	Reference
Identity	$I$	Plain SVD [8, 33]
Diagonal Hessian	$\text{diag}[(XX^\top + \lambda I)^{-1}]^{\frac{-1}{2}}$	OBS [12]; GPTQ [11]; SparseGPT [10]
Diagonal $\ell_1$ -norm	$\text{diag}[\sum_j  X_{1,j} , \dots, \sum_j  X_{d,j} ]^\alpha$	ASVD [47]; AWQ [23]
Diagonal $\ell_2$ -norm	$\text{diag}[XX^\top]^\frac{1}{2}$	WandA [38]
Covariance	$XX^\top + \lambda I$	CorDA [45]
Root-Covariance	$(XX^\top + \lambda I)^\frac{1}{2}$	LatentLLM (Ours)

we use the optimal root covariance:  $P = C^\frac{1}{2}$ . See more discussion in Appendix B.1.

**Remark 2** In the presence of a bias term, the optimal solution is modified accordingly (from auto-correlation to covariance). See Appendix B.2.

**Remark 3** Scaling the covariance has no impact in the performance, and it can be often normalized as  $C = (XX^\top + \lambda I)/l$ .

### 3.3. Junction matrix for model compression

In fact, the solution of Eq. (3) does not have a unique decomposition into low-rank matrices  $B$  and  $A$ . The truncated SVD is written as

$$USV = \text{svd}_r[WP], \quad (6)$$

where  $U \in \mathbb{R}^{d' \times r}$ ,  $S \in \mathbb{R}^{r \times r}$ , and  $V \in \mathbb{R}^{r \times d}$  are the left singular unitary matrix, singular-value diagonal matrix, and right singular unitary matrix, respectively. The decomposition and compression matrices  $B$  and  $A$  can be expressed:

$$B = USJ, \quad A = J^+VP^+, \quad (7)$$

where  $J \in \mathbb{R}^{r \times r}$  is a junction matrix and  $[\cdot]^+$  denotes the pseudo inverse. Choosing any junction matrix that satisfies  $SJJ^+ = S$  has no impact on the loss. Hence, there is few literature discussing the choice of  $J$ . Typically, one may use  $J = I$  to put singular-values into the decompression matrix;  $J = S^+$  to put it into the compression matrix; or  $J = [S^\frac{1}{2}]^+$  to split it across both matrices equally.

However, a certain choice of  $J$  has a noticeable advantage to reduce the number of parameters and floating-point operations (FLOPs). We can write the whitened right-singular matrix  $VP^+$  as two sub-blocks:

$$VP^+ = \begin{bmatrix} V_1 & V_2 \end{bmatrix}, \quad (8)$$

for  $V_1 \in \mathbb{R}^{r \times r}$  and  $V_2 \in \mathbb{R}^{r \times (d-r)}$ . When we use  $J = V_1$ , the compression matrix  $A$  will contain an identity block as long as  $V_1$  is non-singular:

$$A = J^+VP^+ = V_1^+ \begin{bmatrix} V_1 & V_2 \end{bmatrix} = \begin{bmatrix} I & V_1^+V_2 \end{bmatrix}. \quad (9)$$

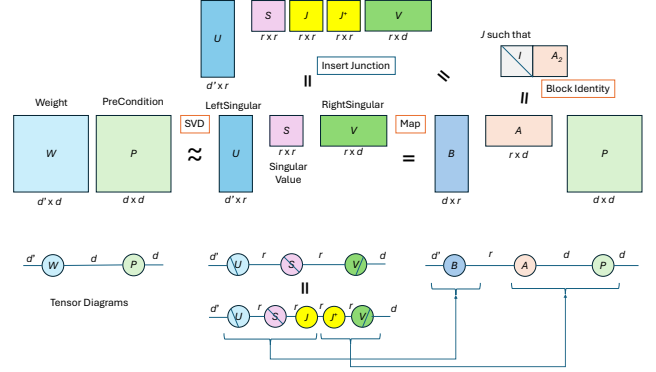


Figure 2. Activation-aware compression with pre-conditioning and junction matrix. The junction matrix  $J$  can be adjusted such that  $A$  or  $B$  is block identity to save the number of parameters and inference computation.

This can greatly reduce the number of parameters from  $r(d' + d)$  to  $r(d' + d) - r^2$ , as well as the FLOPs, because no computation is needed for the identity projection.

For example, when the hidden size is  $d = d'$ , even if we compress it by 25%, i.e., the latent size is  $r = 0.75d$ , the total number of parameters will be  $r(d' + d) = 1.5d^2$ , which is 50% more than the original  $d^2$ . This increased FLOPs hinders the low-rank compression of LLMs, even with the KV cache benefit [5, 24, 47]. Nevertheless, with our identity block form, we can always reduce the number of parameters regardless of the latent size, i.e.,  $r(d' + d) - r^2 < d'd$  for  $r < \min(d', d)$ . For the above example of 25% latent compression, we can achieve  $r(d' + d) - r^2 = (15/16)d^2 < d^2$ .

Fig. 2 depicts the role of the pre-conditioning and junction matrices for the activation-aware compression. We also illustrate the tensor diagrams to understand the flexibility of tensor mapping.

**Remark 4** Pivoting columns can solve the case when the left-most sub-block  $V_1$  is singular. The pivoting does not require any FLOPs in inference while additional memory is required to record the permutation index.

**Remark 5**  $J = V_1$  is not the only useful choice: (i) we can

transform  $B$  into a block-identity form in a similar manner; or (ii) we can nullify the upper triangular of both  $B$  and  $A$  like LU factorization. See more discussion in Appendix A.2.

#### 4. LatentLLM: Joint tensor compression

The SVD described above is optimal in the sense that the local error is minimized for the single tensor compression, whereas it does not guarantee global optimality. Motivated by the global loss minimization framework introduced by SparseLLM [3], we propose a joint tensor compression technique which factorizes multiple tensors in adjacent modules concurrently.

##### 4.1. Multi-head latent attention: Joint QK SVD

First, we consider a joint compression of query (Q) and key (K) projections in MHA to convert into MLA. The attention map is the dot product of query and key features:

$$M_i = X^\top W_{q,i}^\top W_{k,i} X, \quad (10)$$

where  $M_i \in \mathbb{R}^{l \times l}$  is the  $i$ th head attention map before softmax operation,  $W_{q,i} \in \mathbb{R}^{d_h \times d}$  is the  $i$ th head query projection matrix, and  $W_{k,i} \in \mathbb{R}^{d_h \times d}$  is the  $i$ th head key projection matrix. Here,  $d_h$  is the head dimension, which is often  $d_h = d/h$  for the number of heads  $h$ .

Rather than individually compressing Q and K projections, we consider minimizing the attention map error:

$$\mathcal{L}_2 = \sum_{i=1}^h \|M_i - \hat{M}_i\|^2, \quad (11)$$

where  $\hat{M}_i$  is the  $i$ th head latent attention with the low-rank compression:

$$\hat{M}_i = X^\top A_q^\top B_{q,i}^\top B_{k,i} A_k X, \quad (12)$$

where  $A_q \in \mathbb{R}^{r_q \times d}$  is the Q latent compression matrix,  $A_k \in \mathbb{R}^{r_k \times d}$  is the K latent compression matrix,  $B_{q,i} \in \mathbb{R}^{d_h \times r_q}$  is the  $i$ th head Q latent decompression matrix, and  $B_{k,i} \in \mathbb{R}^{d_h \times r_k}$  is the  $i$ th head K latent decompression matrix, respectively. Here,  $r_q$  and  $r_k$  are the latent dimensions for Q and K.

Similar to Eq. (5), we can write

$$\begin{aligned} \mathcal{L}_2 &= \sum_{i=1}^h \left\| \underbrace{C^{\frac{1}{2}} W_{q,i}^\top W_{k,i} C^{\frac{1}{2}}}_{G_i \in \mathbb{R}^{d \times d}} - \underbrace{C^{\frac{1}{2}} A_q^\top}_{A'_q \in \mathbb{R}^{r_q \times d}} \underbrace{B_{q,i}^\top B_{k,i}}_{H_i \in \mathbb{R}^{r_q \times r_k}} \underbrace{A_k C^{\frac{1}{2}}}_{A'_k} \right\|^2 \\ &= \sum_{i=1}^h \|G_i - A'_q H_i A'_k\|^2. \end{aligned} \quad (13)$$

This is known as a high-order SVD (HOSVD) problem to decompose for the 3-mode tensor  $G \in \mathbb{R}^{h \times d \times d}$ , whose  $i$ th

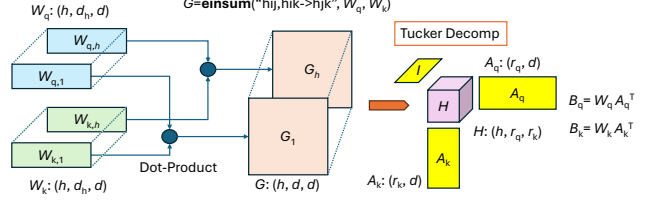


Figure 3. Tucker decomposition for joint QK compression. The compression matrices  $A_q$  and  $A_k$  correspond to the Tucker tensor planes, while  $H = A_q G A_k^\top$  is the Tucker tensor core. For simplicity, we omit junction matrices and pre-conditioning matrix.

slice is  $G_i$ .  $A'_q$  corresponds to the 2nd tensor plane,  $A'_k$  is the 3rd tensor plane, and  $H \in \mathbb{R}^{h \times r_q \times r_k}$ , whose  $i$ th slice is  $H_i$ , is the tensor core. This is illustrated in Fig. 3.

This Tucker tensor decomposition is typically solved by alternating SVD over each slice sequentially. Algorithm 1 shows the pseudo-code of the joint SVD compression for QK latent projections. See the detailed derivations of the joint SVD algorithm in Appendix E. Here, we generalize the pre-conditioning matrix  $P$ , as not necessarily the optimal  $C^{\frac{1}{2}}$ . In addition, we explicitly denoted any arbitrary junction matrices that do not change the error. Note that there are additional junction matrices per heads  $J_i \in \mathbb{R}^{d_h \times d_h}$  as well as individual Q/K junctions  $J_q \in \mathbb{R}^{r_k \times r_k}$  and  $J_k \in \mathbb{R}^{r_k \times r_k}$ . This suggests that we can further reduce the number of parameters by transforming into the block identity form per head. The total number of parameters will be  $(r_q + r_k)(d + d_h h) - r_q^2 - r_k^2 - d_h^2 h$ , reduced from the original weights  $2dd_h h$ .

**Remark 6** This conversion from MHA to MLA with joint QK SVD can be readily applied to grouped query attention (GQA). See Appendix E.3.

**Remark 7** Our joint QK SVD can be extended with most positional encoding methods. See Appendix F.

**Remark 8** A naive way of joint SVD for QKV projections is discussed in Appendix C. We found this to be worse than the joint QK compression described here.

**Remark 9** In the presence of bias terms, the solution is modified slightly. See Appendix E.2.

**Remark 10** Attention-aware pruning [21] is related to our method, while our derivation provides an optimal tensor rank decomposition and only requires preconditioning matrices.



---

**Algorithm 1** Joint SVD for QK Projections in MHA

---

**Input:** Pre-conditioning  $P \in \mathbb{R}^{d \times d}$ , query projection heads  $W_{q,i} \in \mathbb{R}^{d_h \times d}$ , key projection heads  $W_{k,i} \in \mathbb{R}^{d_h \times d}$ , number of heads  $h$ , rank  $r_q, r_k$ , iteration  $N$

**Initialize:**

$$W_{q,i} = W_{q,i} P \text{ for } i \in \{1, \dots, h\}$$

$$W_{k,i} = W_{k,i} P \text{ for } i \in \{1, \dots, h\}$$

$$G_i = W_{q,i}^\top W_{k,i} \text{ for } i \in \{1, \dots, h\}$$

$$A_q = \text{RightSingular}_{r_q} \left[ \sum_{i=1}^h G_i G_i^\top \right]$$

**for**  $n = 1$  **to**  $N$  **do**

$$A_k = \text{RightSingular}_{r_k} \left[ \sum_{i=1}^h G_i^\top A_q^\top A_q G_i \right]$$

$$A_q = \text{RightSingular}_{r_q} \left[ \sum_{i=1}^h G_i A_k A_k^\top G_i^\top \right]$$

**end for**

**Output:**

$$B_{q,i} = J_i^\top W_{q,i} A_q^\top J_q \text{ for } i \in \{1, \dots, h\}$$

$$B_{k,i} = J_i^\top W_{k,i} A_k^\top J_k \text{ for } i \in \{1, \dots, h\}$$

$$A_q = J_q^+ A_q P^+$$

$$A_k = J_k^+ A_k P^+$$


---

## 4.2. Multi-head latent attention: Joint VO SVD

Next, we discuss the joint SVD for value (V) and output (O) projections in MHA. The MHA output can be written as

$$Y' = \sum_{i=1}^h W_{o,i} W_{v,i} X \text{ softmax}[M_i^\top], \quad (14)$$

where  $W_{o,i} \in \mathbb{R}^{d' \times d_h}$  is the  $i$ th head output projection, and  $W_{v,i} \in \mathbb{R}^{d_h \times d}$  is the  $i$ th head value value projection. For any arbitrary attention map, we may consider minimizing the loss:

$$\mathcal{L}_3 = \sum_{i=1}^h \|W_{o,i} W_{v,i} X - \hat{W}_{o,i} \hat{W}_{v,i} X\|^2, \quad (15)$$

for the low-rank compression:  $\hat{W}_{o,i} = B_o A_{o,i} \in \mathbb{R}^{d' \times d_h}$  and  $\hat{W}_{v,i} = B_{v,i} A_v \in \mathbb{R}^{d_h \times d}$  with  $B_o \in \mathbb{R}^{d' \times r_o}$ ,  $A_{o,i} \in \mathbb{R}^{r_o \times d_h}$ ,  $B_{v,i} \in \mathbb{R}^{d_h \times r_v}$ , and  $A_v \in \mathbb{R}^{r_v \times d}$ . The MLA output is thus given as

$$\hat{Y}' = \sum_{i=1}^h B_o A_{o,i} B_{v,i} A_v X \text{ softmax}[M_i]. \quad (16)$$

Interestingly, this is also formulated in a similar manner of Eq. (13), and it can be solved by the joint SVD algorithm.

Note that the MLA computations can be more efficient depending on tensor contraction ordering. Specifically, Eq. (16) requires complexity of  $\mathcal{O}[ldr_v + hd_d lr_v + hd_h l^2 + hd_h lr_o + hdlr_o]$  in the order:

$$\hat{Y}' = \sum_{i=1}^h \left( B_o \left( A_{o,i} \left( (B_{v,i} (A_v X)) \text{ softmax}[M_i] \right) \right) \right). \quad (17)$$

It can be reduced by computing in another order:

$$\hat{Y}' = B_o \sum_{i=1}^h \left( A_{o,i} \left( B_{v,i} \left( (A_v X) \text{ softmax}[M_i] \right) \right) \right), \quad (18)$$

which requires complexity of  $\mathcal{O}[ldr_v + r_v l^2 + hd_h lr_v + hd_h lr_o + dlr_o]$ . The reduction is  $\mathcal{O}[(d-r_v)l^2 + (h-1)dlr_o]$ . If  $hr_o < r_v$ , then the attention weighting should be done on output compression  $A_{o,i}$ .

**Remark 11** *Because the above loss does not deal with the nonlinear attention map, it was found that the joint VO compression was not effective over the split V/O compression. Nonetheless, we derived several different alternatives. See Appendix G.*

## 4.3. Latent MLP: Joint UD SVD

Finally, we address the joint compression of MLP layers which consists of up (U) projection and down (D) projection in typical LLMs/LMMs. Although the global optimization is generally difficult due to the nonlinear activations in the MLP layer, SparseLLM [3] provides an elegant way to approximate MLP layer. The key idea is to minimize the MLP loss in a decoupled manner by introducing auxiliary variables. Our LatentLLM exploits the same philosophy to compress MLP layers.

Consider a 2-layer MLP:

$$Z = W_u X, \quad Z' = \sigma(Z), \quad Y = W_d Z', \quad (19)$$

where  $W_u \in \mathbb{R}^{d_i \times d}$  is the up projection matrix,  $W_d \in \mathbb{R}^{d \times d_i}$  is the down projection matrix, and  $d_i$  is the intermediate size which is typically four-fold of hidden size:  $d_i = 4d$ . The intermediate variables  $Z, Z' \in \mathbb{R}^{d_i \times l}$  are auxiliary factors to be optimized.

Specifically, we consider minimizing the decoupled loss:

$$\mathcal{L}_4 = \alpha \|W_u X - Z\|^2 + \beta \|Z' - \sigma(Z)\|^2 + \gamma \|W_d Z' - Y\|^2, \quad (20)$$

for auxiliary variables  $Z$  and  $Z'$ , given calibration input  $X$  and output  $Y$ .

Following SparseLLM [3], the optimal  $Z'$  can be obtained given the other parameters fixed:

$$Z' = (\gamma W_d^\top W_d + \beta I)^+ (\beta \sigma(Z) + \gamma W_d^\top Y). \quad (21)$$

The optimal  $Z$  can be also obtained in closed-form for the case of ReLU:

$$Z_- = W_u X, \quad Z_+ = \frac{1}{\alpha + \beta} (\alpha Z_- + \beta Z'), \quad (22)$$

depending on  $Z$ 's element-wise sign.

Table 2. Perplexity ( $\downarrow$ ) of OPT models with different SVD compression methods for 10–40% size reduction. Asterisk “\*” indicates the better performance than the original un-compressed LLM.

Compression	10%			20%			30%			40%		
Dataset	WT2	PTB	C4	WT2	PTB	C4	WT2	PTB	C4	WT2	PTB	C4
OPT-125M (WT2: 27.7, PTB: 39.0, C4: 26.6)												
Plain SVD (Identity)	393.8	608.8	274.6	668.9	1098.0	559.0	1298.3	1888.7	806.5	3306.5	2985.9	1637.0
ASVD (Hessian)	57.8	92.8	45.0	106.9	169.8	79.9	288.1	530.4	215.0	838.9	1581.9	608.2
ASVD ( $\ell_2$ -norm)	49.7	74.7	42.2	87.3	126.8	72.0	256.0	282.1	188.3	906.9	864.3	528.4
ASVD (Cov)	87.5	121.5	67.6	115.7	157.0	83.1	163.1	242.8	109.9	248.3	390.6	158.4
ASVD (RootCov)	40.5	64.4	34.5	54.8	86.8	42.7	88.8	148.9	61.5	177.5	306.7	116.8
LatentLLM (RootCov)	<b>29.0</b>	<b>42.3</b>	<b>27.6</b>	<b>32.9</b>	<b>50.9</b>	<b>30.4</b>	<b>43.4</b>	<b>68.7</b>	<b>37.4</b>	<b>73.4</b>	<b>68.7</b>	<b>37.4</b>
OPT-350M (WT2: 22.0, PTB: 31.1, C4: 22.6)												
Plain SVD (Identity)	112.3	130.8	82.8	211.3	226.8	151.5	378.1	392.0	258.7	705.5	635.5	509.8
ASVD (Hessian)	64.0	89.1	50.9	104.6	134.4	80.3	202.1	212.0	145.9	557.3	558.6	371.6
ASVD ( $\ell_2$ -norm)	40.0	59.9	36.6	59.4	78.0	49.8	117.5	134.2	86.9	308.7	283.9	201.1
ASVD (Cov)	78.0	90.6	61.7	100.8	111.0	72.7	311.2	356.8	129.4	1485.3	922.7	548.2
ASVD (RootCov)	30.8	42.2	28.5	39.0	51.4	33.6	71.6	86.1	49.5	118.5	132.1	73.0
LatentLLM (RootCov)	<b>23.1</b>	<b>33.3</b>	<b>23.6</b>	<b>25.9</b>	<b>37.0</b>	<b>25.8</b>	<b>32.9</b>	<b>45.0</b>	<b>30.6</b>	<b>51.3</b>	<b>63.4</b>	<b>42.5</b>
OPT-1.3B (WT2: 14.6, PTB: 20.3, C4: 16.1)												
Plain SVD (Identity)	9428.1	10670.8	4865.4	16461.2	20589.0	11039.8	18105.3	17360.8	12565.2	22155.9	15820.3	16566.2
ASVD (Hessian)	23.8	40.6	24.9	63.0	173.7	52.8	825.8	927.9	385.0	4912.3	3086.3	2138.9
ASVD ( $\ell_2$ -norm)	20.3	32.3	21.6	28.7	60.2	27.7	74.5	217.4	58.5	592.4	1072.0	336.7
ASVD (Cov)	29750.9	31499.1	18646.3	19716.9	21757.2	14967.2	21738.3	24300.2	16428.7	22776.5	23591.7	14922.1
ASVD (RootCov)	17.7	27.9	18.9	21.9	35.3	22.2	33.9	55.8	29.7	75.0	107.9	51.1
LatentLLM (RootCov)	<b>*14.5</b>	<b>21.5</b>	<b>16.6</b>	<b>15.8</b>	<b>24.3</b>	<b>17.8</b>	<b>20.2</b>	<b>31.6</b>	<b>21.3</b>	<b>34.1</b>	<b>58.1</b>	<b>30.6</b>
OPT-2.7B (WT2: 12.5, PTB: 18.0, C4: 14.3)												
Plain SVD (Identity)	1922.0	2250.3	900.7	7446.2	7042.4	5113.6	11253.8	10109.6	7742.6	26177.5	29321.3	17035.3
ASVD (Hessian)	18.2	31.9	20.0	31.6	96.9	28.0	216.2	852.3	74.8	2714.9	2894.0	626.0
ASVD ( $\ell_2$ -norm)	16.9	27.1	18.7	23.1	44.6	23.4	53.0	190.7	43.2	524.3	981.5	229.3
ASVD (Cov)	16419.9	15136.0	10680.6	15495.8	14896.4	10891.6	17392.3	15994.8	11926.0	17976.5	16298.1	11566.8
ASVD (RootCov)	14.5	22.1	16.5	17.1	26.7	18.8	24.1	36.3	23.7	48.4	66.5	37.1
LatentLLM (RootCov)	<b>*12.3</b>	<b>18.8</b>	<b>14.7</b>	<b>13.6</b>	<b>20.6</b>	<b>15.7</b>	<b>16.5</b>	<b>24.3</b>	<b>18.1</b>	<b>24.5</b>	<b>36.0</b>	<b>24.2</b>
OPT-6.7B (WT2: 10.9, PTB: 15.8, C4: 12.7)												
Plain SVD (Identity)	14839.0	28665.9	22936.1	67517.7	116974.8	110860.5	123286.4	213333.5	190378.4	27304.0	31719.7	24071.3
ASVD (Hessian)	14.3	22.0	16.6	17.3	27.3	20.1	26.0	51.0	28.8	73.3	252.2	67.6
ASVD ( $\ell_2$ -norm)	12.6	19.6	15.1	14.6	23.0	17.2	18.7	32.1	21.4	30.6	73.2	33.7
ASVD (Cov)	9111.6	9171.3	7220.2	9842.6	9465.6	7175.0	11848.0	10046.0	6973.6	8514.7	7931.2	6660.3
ASVD (RootCov)	11.8	17.7	14.2	13.5	19.5	15.4	17.0	23.9	17.8	27.2	36.1	24.0
LatentLLM (RootCov)	<b>*10.7</b>	<b>16.1</b>	<b>13.0</b>	<b>11.5</b>	<b>17.4</b>	<b>13.7</b>	<b>13.5</b>	<b>19.2</b>	<b>15.3</b>	<b>18.0</b>	<b>24.2</b>	<b>18.4</b>
OPT-13B (WT2: 10.1, PTB: 14.5, C4: 12.1)												
Plain SVD (Identity)	892.2	1003.5	789.3	2157.4	2068.3	1716.1	3612.9	3381.8	2806.9	5838.7	5069.1	4292.5
ASVD (Hessian)	12.5	18.6	14.3	14.6	22.0	15.8	19.1	29.7	18.7	29.5	48.9	25.1
ASVD ( $\ell_2$ -norm)	11.2	16.8	13.4	12.2	18.6	14.4	14.0	21.9	16.3	18.2	29.0	20.3
ASVD (Cov)	13999.3	11053.5	8991.2	10250.7	8883.2	6556.4	12885.3	11756.7	7658.0	12625.5	10709.9	7972.3
ASVD (RootCov)	10.9	15.9	13.1	11.9	17.0	13.9	14.3	20.0	15.3	20.2	24.1	18.3
LatentLLM (RootCov)	<b>10.2</b>	<b>14.8</b>	<b>12.4</b>	<b>10.7</b>	<b>15.4</b>	<b>13.0</b>	<b>12.0</b>	<b>16.7</b>	<b>13.9</b>	<b>14.8</b>	<b>19.2</b>	<b>15.8</b>

This approach can be used for low-rank approximation.

Given  $Z$ , we can optimize low-rank matrix  $\hat{W}_u = B_u A_u$  by

SVD of  $ZX^+C_d^{\frac{1}{2}}$ , where  $ZX^+$  corresponds to the effective weight matrix to map  $X$  onto  $Z$ . Given  $Z'$ , we approximate  $\hat{W}_d = B_d A_d$  by SVD of  $Y Z'^+ C_d^{\frac{1}{2}}$ , given correlation  $C_d = Z' Z'^T$ . This alternating solution is iterated over a few rounds. For detail, see Appendix H.

## 5. Experiments

**Experiments setup** We conduct experiments for LLM and LMM benchmarks to evaluate the effectiveness of our method. Our experiments are based on the same setting of SparseLLM [3] and their code base<sup>1</sup>. We implemented LatentLLM in PyTorch [29] and used the HuggingFace Transformers library [43] for handling models and datasets. All experiments are conducted on NVIDIA A40 GPUs.

For LLM calibration data, we follow the same setup of [10] and use 64 samples of 2048-token segments, randomly chosen from the first shard of the C4 [31] dataset. This dataset represents generic text data crawled from the internet and ensures our experiments are zero-shot as no task-specific data is seen during compression. We followed existing work [38] and compressed all linear layers in MLP and MHA in LLMs to the target compression ratio. For LMM calibration data, we use 64 samples, randomly chosen from the train split of the ScienceQA [26] multi-modal question answering dataset.

**Models and datasets** For LLM experiments, we consider the OPT model family [49] as it provides a wide range of model scales from 125M to 175B as noted in Appendix J. We show results on different sizes of models to provide a broader picture for the performance of LatentLLM. In terms of metrics, we mainly focus on perplexity, which is known to be a challenging and stable metric that is well-suited for evaluating the accuracy of compression methods [9, 46]. We consider the test sets of raw-WikiText2 (WT2) [28] and the Penn Treebank (PTB) [27] as well as a subset of the C4 validation data, all popular benchmarks in the LLM compression literature [10, 11, 38].

For LMM experiments, we use LLaVa [25], specifically liuhaotian/llava-v1.6-vicuna-7b model, which consists of language transformer based on Vicuna and vision transformer (ViT) based on the contrastive language-image pre-training (CLIP). We evaluate the capability of the multi-modal answer reasoning based on the ScienceQA dataset, which contains 21K vision-language multi-choice questions for three subjects: natural, social, and language science. Some fractions of questions have image and/or text contexts, and the problem levels range from grade 1 to 12.

<sup>1</sup><https://github.com/BaiTheBest/SparseLLM>

Table 3. Computational complexity of OPT-6.7B models compressed by LatentLLM.

Compression	FLOPs	MACs	Parameters
0%	1.70T	851G	6.66B
10%	1.53T	766G	6.20B
20%	1.36T	681G	5.53B
30%	1.19T	596G	4.87B
40%	1.02T	511G	4.20B
50%	851G	425G	3.54B
60%	681G	340G	2.87B
70%	511G	255G	2.21B
80%	341G	170G	1.54B
90%	171G	85.2G	880M

**Baseline methods** We compare our LatentLLM against several baselines: weight-based plain SVD compression applied locally, and several variants of local ASVD compression with different pre-conditioning matrix as listed in Tab. 1.

**Computational complexity** When all linear modules are compressed with LatentLLM, the inference complexity is expected to be reduced with the compression ratio almost linearly. Nevertheless LLMs/VLMs have extra complexity other than linear affine transforms, the inference complexity is not precisely proportional to the compression factor. We show the complexity analysis in Tab. 3 for the compressed OPT-6.7B models, based on the `calcflops`<sup>2</sup> library. We assume the token length of 128 for FLOPs analysis. We found that the FLOPs, multiply-accumulation operations (MACs), and parameters are almost linearly reduced with the compression factor.

**Compression over model size** We first look into the compression capabilities of our LatentLLM across various model sizes in comparison to baseline methods. Detailed results are shown for a size reduction over 10–40% in Tab. 2, and wider visualization in Fig. 4. The perplexity results of the original un-compressed LLM models are reported next to the names of the models in the table.

We can see that the conventional plain SVD has a poor performance, and that ASVD with a proper pre-conditioning can significantly improve the perplexity. It was found that the diagonal Hessian is worse than the diagonal  $\ell_2$ -norm, whereas covariance pre-conditioning can be terrible in low compression regimes for larger LLMs. In contrast, the superiority of root covariance is remarkable. More importantly, our block identity transform is considerably beneficial to compress LLMs. In addition, the joint

<sup>2</sup><https://pypi.org/project/calcflops/>

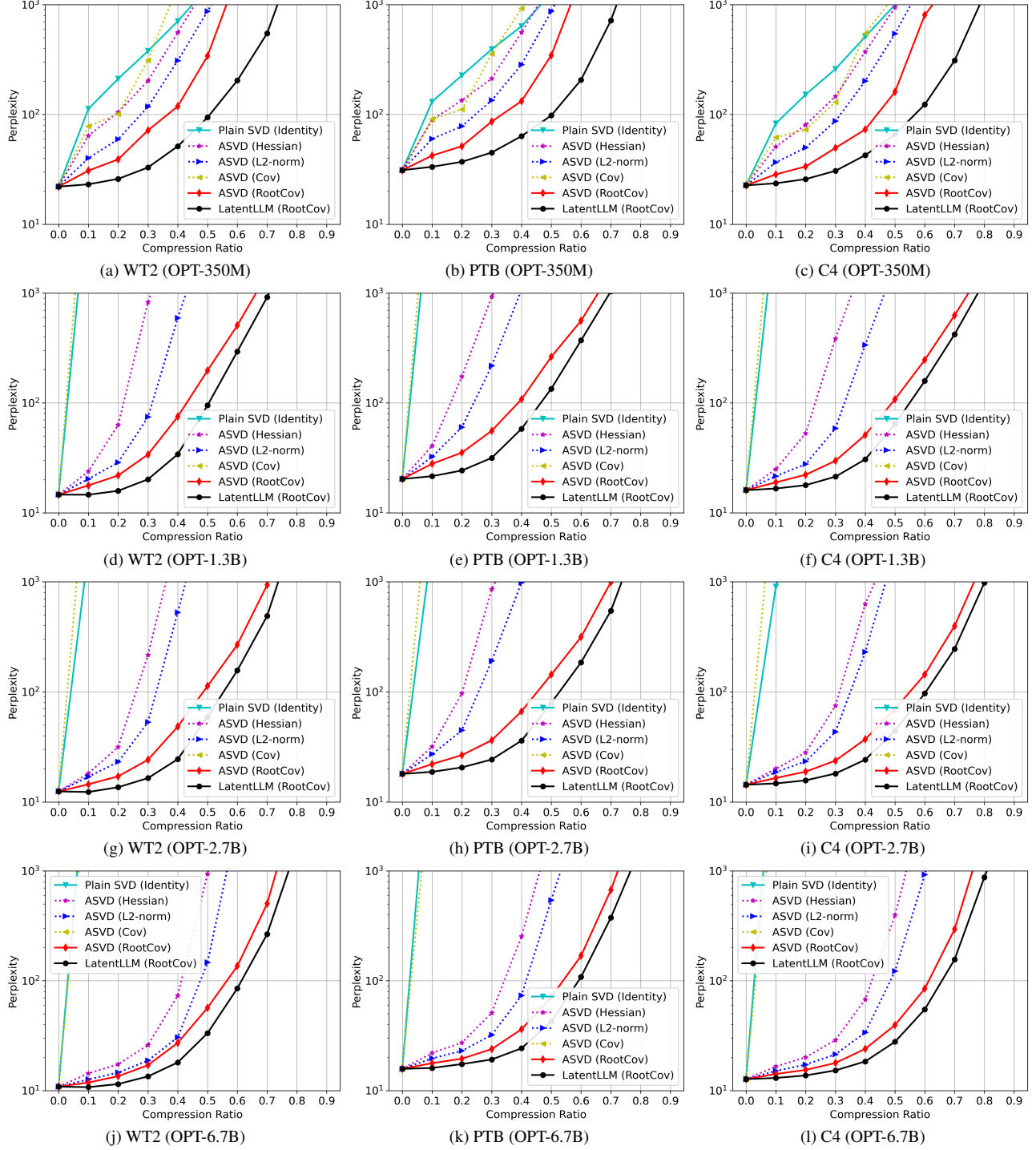


Figure 4. Perplexity over compression ratio for OPT models.

SVD used for LatentLLM offers an additional improvement for the most cases. For LatentLLM, we used 4 iterations for joint UD compression and 8 iterations for joint QK compression. Notice that our methods can also achieve slightly better performance than the original un-compressed LLMs

for a few cases.

**Multi-modal reasoning capability** We show the accuracy of latent LLaVa models for ScienceQA multi-modal reasoning benchmark in Tab. 4. It is verified that our La-

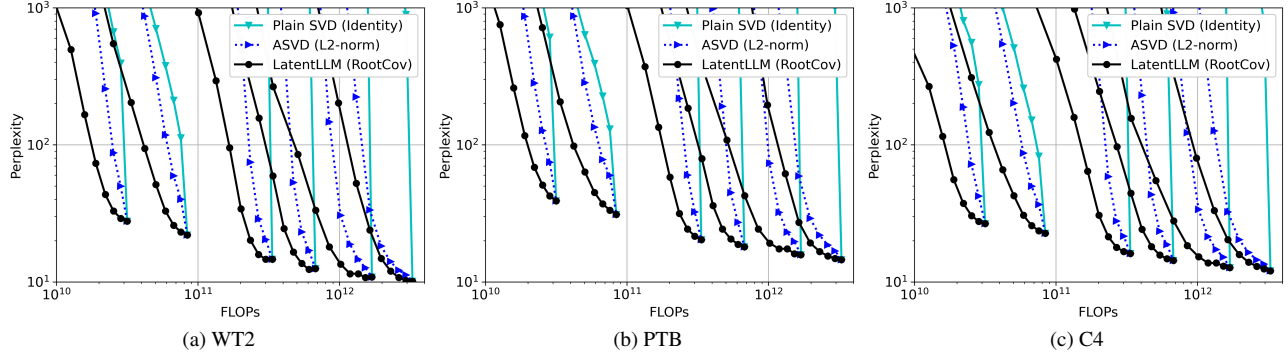


Figure 5. Perplexity vs. FLOPs of compressed OPT for 125M to 13B models.

tentLLM can significantly outperform other low-rank compression methods across diverse reasoning problems over different subjects/contexts/grades, approaching the performance of the original un-compressed LLaVa model. Fig. 6 shows the corresponding radar plots at 10%–50% compressions. It is seen that ASVD without using proper pre-conditioning matrix degrades the performance quickly with higher compression ratios, while our LatentLLM keeps relatively higher performance across all cases. Also, we observe that context-less, language science, and higher grade questions tend to have lower performance.

**Discussion** Our framework with optimal pre-conditioning and joint Q/K, V/O distillations can be readily applied to pruning and quantization as well. See some results and discussion in Appendix I and Appendix I.1. Further fine-tuning is expected to be able to compensate for the performance degradation by the latent reduction.

## 6. Summary

We introduced LatentLLM which jointly compresses multiple tensors through the use of high-order tensor-rank decomposition. We also provided some new perspectives for activation-aware compression when choosing the pre-conditioner and junction matrix. With a proper selection, we demonstrated that the model compression performance can be significantly improved. Our latent LLaVa showed a significant advantage in multi-modal reasoning tasks compared to other baseline methods.

## References

- [1] Josh Achiam, Steven Adler, Sandhini Agarwal, Lama Ahmad, Ilge Akkaya, Florencia Leoni Aleman, Diogo Almeida, Janko Altenschmidt, Sam Altman, Shyamal Anadkat, et al. GPT-4 technical report. *arXiv preprint arXiv:2303.08774*, 2023. 1
- [2] Guangji Bai, Zheng Chai, Chen Ling, Shiyu Wang, Jiaying Lu, Nan Zhang, Tingwei Shi, Ziyang Yu, Mengdan Zhu,
- Yifei Zhang, et al. Beyond efficiency: A systematic survey of resource-efficient large language models. *arXiv preprint arXiv:2401.00625*, 2024. 1
- [3] Guangji Bai, Yijiang Li, Chen Ling, Kibaek Kim, and Liang Zhao. SparseLLM: Towards global pruning of pre-trained language models. In *The Thirty-eighth Annual Conference on Neural Information Processing Systems*, 2024. 1, 2, 4, 5, 7, 31, 33
- [4] Sébastien Bubeck, Varun Chandrasekaran, Ronen Eldan, Johannes Gehrke, Eric Horvitz, Ece Kamar, Peter Lee, Yin Tat Lee, Yuanzhi Li, Scott Lundberg, et al. Sparks of artificial general intelligence: Early experiments with GPT-4. *arXiv preprint arXiv:2303.12712*, 2023. 1
- [5] Chi-Chih Chang, Wei-Cheng Lin, Chien-Yu Lin, Chong-Yan Chen, Yu-Fang Hu, Pei-Shuo Wang, Ning-Chi Huang, Luis Ceze, Mohamed S Abdelfattah, and Kai-Chiang Wu. Palu: Compressing KV-cache with low-rank projection. *arXiv preprint arXiv:2407.21118*, 2024. 1, 2, 3
- [6] Zihang Dai, Zhilin Yang, Yiming Yang, Jaime Carbonell, Quoc V Le, and Ruslan Salakhutdinov. Transformer-XL: Attentive language models beyond a fixed-length context. *arXiv preprint arXiv:1901.02860*, 2019. 26
- [7] DeepSeek-AI, Daya Guo, Dejian Yang, Haowei Zhang, Junxiao Song, Ruoyu Zhang, Runxin Xu, Qihao Zhu, Shitong Ma, Peiyi Wang, Xiao Bi, Xiaokang Zhang, Xingkai Yu, Yu Wu, Z. F. Wu, Zhibin Gou, Zhihong Shao, Zhuoshu Li, Ziyi Gao, Aixin Liu, Bing Xue, Bingxuan Wang, Bochao Wu, Bei Feng, Chengda Lu, Chenggang Zhao, Chengqi Deng, Chenyu Zhang, Chong Ruan, Damai Dai, Deli Chen, Dongjie Ji, Erhang Li, Fangyun Lin, Fucong Dai, Fuli Luo, Guangbo Hao, Guanting Chen, Guowei Li, H. Zhang, Han Bao, Hanwei Xu, Haocheng Wang, Honghui Ding, Huajian Xin, Huazuo Gao, Hui Qu, Hui Li, Jianzhong Guo, Jiashi Li, Jiawei Wang, Jingchang Chen, Jingyang Yuan, Junjie Qiu, Junlong Li, J. L. Cai, Jiaqi Ni, Jian Liang, Jin Chen, Kai Dong, Kai Hu, Kaige Gao, Kang Guan, Kexin Huang, Kuai Yu, Lean Wang, Lecong Zhang, Liang Zhao, Litong Wang, Liyue Zhang, Lei Xu, Leyi Xia, Mingchuan Zhang, Minghua Zhang, Minghui Tang, Meng Li, Miaoqun Wang, Mingming Li, Ning Tian, Panpan Huang, Peng Zhang, Qiancheng Wang, Qinyu Chen, Qiushi Du, Ruiqi Ge, Ruisong Zhang, Ruizhe Pan, Runji Wang, R. J. Chen, R. L. Jin, Ruyi Chen,



Table 4. Accuracy in percent ( $\uparrow$ ) on ScienceQA dataset of LLaVa model with different compression methods for 10%–50% size reduction. Question subjects: natural science (NAT); social science (SOC); language science (LAN). Context modality: text (TXT); image (IMG); or no context (NO). Grades: 1–6 (G1-6); 7–12 (G7-12).

Method	Compression	Subject			Context Modality			Grades		Avg
		NAT	SOC	LAN	TXT	IMG	NO	G1-6	G7-12	
Original un-compressed	0%	72.47	69.18	65.73	73.51	68.82	65.99	72.72	65.19	70.03
Plain SVD (Identity)	10%	5.33	1.35	0.27	5.77	6.69	0.00	3.30	2.97	3.18
ASVD (Hessian)	10%	17.23	24.97	3.18	18.43	29.55	2.16	17.40	11.27	15.21
ASVD ( $\ell_2$ -norm)	10%	16.70	18.34	2.55	17.89	24.34	2.23	16.04	8.57	13.37
ASVD (Cov)	10%	41.21	27.22	37.91	41.30	35.15	38.33	38.62	35.27	37.42
ASVD (RootCov)	10%	64.08	56.13	57.36	64.03	60.98	57.35	62.70	57.02	60.67
LatentLLM (RootCov)	10%	<b>68.52</b>	<b>64.23</b>	<b>61.36</b>	<b>69.06</b>	<b>65.20</b>	<b>61.53</b>	<b>68.72</b>	<b>60.45</b>	<b>65.76</b>
Plain SVD (Identity)	20%	0.18	0.00	0.00	0.20	0.20	0.00	0.04	0.20	0.09
ASVD (Hessian)	20%	3.82	2.81	0.00	3.62	5.30	0.14	3.01	1.91	2.62
ASVD ( $\ell_2$ -norm)	20%	0.44	0.79	0.00	0.39	0.79	0.07	0.51	0.20	0.40
ASVD (Cov)	20%	41.39	27.22	37.55	41.45	35.35	38.12	38.69	35.14	37.42
ASVD (RootCov)	20%	61.19	53.43	53.36	61.53	59.40	52.68	58.96	54.98	57.53
LatentLLM (RootCov)	20%	<b>66.39</b>	<b>61.19</b>	<b>60.82</b>	<b>67.20</b>	<b>63.41</b>	<b>60.62</b>	<b>66.41</b>	<b>59.26</b>	<b>63.85</b>
Plain SVD (Identity)	30%	0.13	0.00	0.00	0.10	0.00	0.07	0.11	0.00	0.07
ASVD (Hessian)	30%	0.00	0.00	0.00	0.00	0.00	0.00	0.00	0.00	0.00
ASVD ( $\ell_2$ -norm)	30%	0.09	0.00	0.00	0.10	0.10	0.00	0.04	0.07	0.05
ASVD (Cov)	30%	41.25	27.33	37.36	41.40	35.25	37.84	38.47	35.27	37.33
ASVD (RootCov)	30%	56.66	51.18	52.27	56.74	56.27	51.99	55.73	51.94	54.37
LatentLLM (RootCov)	30%	<b>64.03</b>	<b>56.24</b>	<b>55.27</b>	<b>64.47</b>	<b>61.77</b>	<b>55.40</b>	<b>62.78</b>	<b>55.37</b>	<b>60.13</b>
Plain SVD (Identity)	40%	0.00	0.00	0.00	0.00	0.00	0.00	0.00	0.00	0.00
ASVD (Hessian)	40%	0.04	0.00	0.54	0.05	0.00	0.42	0.07	0.33	0.17
ASVD ( $\ell_2$ -norm)	40%	0.00	0.00	0.27	0.00	0.00	0.21	0.07	0.07	0.07
ASVD (Cov)	40%	40.94	27.22	36.91	41.06	35.10	37.49	38.25	34.81	37.02
ASVD (RootCov)	40%	55.37	49.04	48.36	55.62	54.54	48.50	54.19	48.71	52.23
LatentLLM (RootCov)	40%	<b>56.62</b>	<b>51.07</b>	<b>53.27</b>	<b>56.74</b>	<b>56.12</b>	<b>52.47</b>	<b>55.51</b>	<b>52.93</b>	<b>54.59</b>
Plain SVD (Identity)	50%	0.00	0.00	0.00	0.00	0.00	0.00	0.00	0.00	0.00
ASVD (Hessian)	50%	0.00	0.00	0.00	0.00	0.00	0.00	0.00	0.00	0.00
ASVD ( $\ell_2$ -norm)	50%	0.00	0.00	0.00	0.00	0.00	0.00	0.00	0.00	0.00
ASVD (Cov)	50%	40.94	26.88	36.91	41.20	35.10	37.28	38.18	34.74	36.95
ASVD (RootCov)	50%	52.58	45.11	46.00	52.93	50.07	45.99	51.28	45.75	49.30
LatentLLM (RootCov)	50%	<b>55.55</b>	<b>47.24</b>	<b>49.55</b>	<b>56.01</b>	<b>54.09</b>	<b>48.78</b>	<b>54.55</b>	<b>48.12</b>	<b>52.25</b>

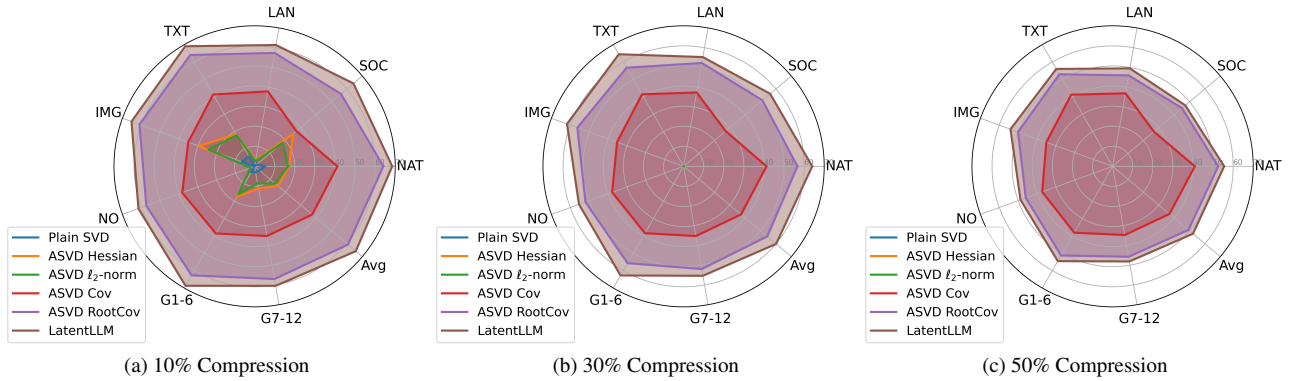


Figure 6. Radar plots of ScienceQA accuracy results across different subjects, context modalities, and grades at 10%–50% compressions.

- Shanghao Lu, Shangyan Zhou, Shanhuang Chen, Shengfeng Ye, Shiyu Wang, Shuiping Yu, Shunfeng Zhou, Shuting Pan, S. S. Li, Shuang Zhou, Shaoqing Wu, Shengfeng Ye, Tao Yun, Tian Pei, Tianyu Sun, T. Wang, Wangding Zeng, Wanjia Zhao, Wen Liu, Wenfeng Liang, Wenjun Gao, Wenqin Yu, Wentao Zhang, W. L. Xiao, Wei An, Xiaodong Liu, Xiaohan Wang, Xiaokang Chen, Xiaotao Nie, Xin Cheng, Xin Liu, Xin Xie, Xingchao Liu, Xinyu Yang, Xinyuan Li, Xuecheng Su, Xuheng Lin, X. Q. Li, Xiangyue Jin, Xiaojin Shen, Xiaosha Chen, Xiaowen Sun, Xiaoxiang Wang, Xinnan Song, Xinyi Zhou, Xianzu Wang, Xinxia Shan, Y. K. Li, Y. Q. Wang, Y. X. Wei, Yang Zhang, Yanhong Xu, Yao Li, Yao Zhao, Yaofeng Sun, Yaohui Wang, Yi Yu, Yichao Zhang, Yifan Shi, Yiliang Xiong, Ying He, Yishi Piao, Yisong Wang, Yixuan Tan, Yiyang Ma, Yiyuan Liu, Yongqiang Guo, Yuan Ou, Yuduan Wang, Yue Gong, Yuheng Zou, Yujia He, Yunfan Xiong, Yuxiang Luo, Yuxiang You, Yuxuan Liu, Yuyang Zhou, Y. X. Zhu, Yanhong Xu, Yanping Huang, Yaohui Li, Yi Zheng, Yuchen Zhu, Yunxian Ma, Ying Tang, Yukun Zha, Yuting Yan, Z. Z. Ren, Zehui Ren, Zhangli Sha, Zhe Fu, Zhean Xu, Zhenda Xie, Zhengyan Zhang, Zhewen Hao, Zhicheng Ma, Zhigang Yan, Zhiyu Wu, Zihui Gu, Zijia Zhu, Zijun Liu, Zilin Li, Ziwei Xie, Ziyang Song, Zizheng Pan, Zhen Huang, Zhipeng Xu, Zhongyu Zhang, and Zhen Zhang. DeepSeek-R1: Incentivizing reasoning capability in LLMs via reinforcement learning, 2025. [1](#)
- [8] Emily L Denton, Wojciech Zaremba, Joan Bruna, Yann LeCun, and Rob Fergus. Exploiting linear structure within convolutional networks for efficient evaluation. *Advances in neural information processing systems*, 27, 2014. [2](#), [3](#)
- [9] Tim Dettmers and Luke Zettlemoyer. The case for 4-bit precision: k-bit inference scaling laws. In *International Conference on Machine Learning*, pages 7750–7774. PMLR, 2023. [7](#)
- [10] Elias Frantar and Dan Alistarh. SparseGPT: Massive language models can be accurately pruned in one-shot. In *International Conference on Machine Learning*, pages 10323–10337. PMLR, 2023. [1](#), [3](#), [7](#), [14](#), [33](#)
- [11] Elias Frantar, Saleh Ashkboos, Torsten Hoefer, and Dan Alistarh. GPTQ: Accurate post-training quantization for generative pre-trained transformers. *arXiv preprint arXiv:2210.17323*, 2022. [1](#), [3](#), [7](#), [14](#)
- [12] Babak Hassibi, David G Stork, and Gregory J Wolff. Optimal brain surgeon and general network pruning. In *IEEE international conference on neural networks*, pages 293–299. IEEE, 1993. [1](#), [3](#), [14](#)
- [13] Cheng-Yu Hsieh, Chun-Liang Li, Chih-Kuan Yeh, Hootan Nakhost, Yasuhisa Fujii, Alexander Ratner, Ranjay Krishna, Chen-Yu Lee, and Tomas Pfister. Distilling step-by-step! outperforming larger language models with less training data and smaller model sizes. *arXiv preprint arXiv:2305.02301*, 2023. [1](#)
- [14] Injoon Hwang, Haewon Park, Youngwan Lee, Jooyoung Yang, and SunJae Maeng. PC-LoRA: Low-rank adaptation for progressive model compression with knowledge distillation. *arXiv preprint arXiv:2406.09117*, 2024. [1](#)
- [15] Albert Q Jiang, Alexandre Sablayrolles, Antoine Roux, Arthur Mensch, Blanche Savary, Chris Bamford, Devendra Singh Chaplot, Diego de las Casas, Emma Bou Hanna, Florian Bressand, et al. Mixtral of experts. *arXiv preprint arXiv:2401.04088*, 2024. [1](#)
- [16] Daniel Martin Katz, Michael James Bommarito, Shang Gao, and Pablo Arredondo. GPT-4 passes the bar exam. *Philosophical Transactions of the Royal Society A*, 382(2270): 20230254, 2024. [1](#)
- [17] Jacob Devlin Ming-Wei Chang Kenton and Lee Kristina Toutanova. BERT: Pre-training of deep bidirectional transformers for language understanding. In *Proceedings of naacL-HLT*, page 2. Minneapolis, Minnesota, 2019. [26](#)
- [18] Yann LeCun, John Denker, and Sara Solla. Optimal brain damage. *Advances in neural information processing systems*, 2, 1989. [1](#)
- [19] Olivier Ledoit and Michael Wolf. A well-conditioned estimator for large-dimensional covariance matrices. *Journal of multivariate analysis*, 88(2):365–411, 2004. [2](#)
- [20] Yixiao Li, Yifan Yu, Qingru Zhang, Chen Liang, Pengcheng He, Weizhu Chen, and Tuo Zhao. LoSparse: Structured compression of large language models based on low-rank and sparse approximation. In *International Conference on Machine Learning*, pages 20336–20350. PMLR, 2023. [2](#)
- [21] Yingyu Liang, Jiangxuan Long, Zhenmei Shi, Zhao Song, and Yufa Zhou. Beyond linear approximations: A novel pruning approach for attention matrix. *arXiv preprint arXiv:2410.11261*, 2024. [4](#)
- [22] Bin Lin, Zhenyu Tang, Yang Ye, Jiayi Cui, Bin Zhu, Peng Jin, Junwu Zhang, Munan Ning, and Li Yuan. MoE-LLaVa: Mixture of experts for large vision-language models. *arXiv preprint arXiv:2401.15947*, 2024. [1](#)
- [23] Ji Lin, Jiaming Tang, Haotian Tang, Shang Yang, Wei-Ming Chen, Wei-Chen Wang, Guangxuan Xiao, Xingyu Dang, Chuang Gan, and Song Han. AWQ: Activation-aware weight quantization for on-device LLM compression and acceleration. *Proceedings of Machine Learning and Systems*, 6:87–100, 2024. [1](#), [3](#), [14](#)
- [24] Aixin Liu, Bei Feng, Bing Xue, Bingxuan Wang, Bochao Wu, Chengda Lu, Chenggang Zhao, Chengqi Deng, Chenyu Zhang, Chong Ruan, et al. DeepSeek-v3 technical report. *arXiv preprint arXiv:2412.19437*, 2024. [1](#), [2](#), [3](#), [13](#)
- [25] Haotian Liu, Chunyuan Li, Qingyang Wu, and Yong Jae Lee. Visual instruction tuning, 2023. [1](#), [7](#)
- [26] Pan Lu, Swaroop Mishra, Tony Xia, Liang Qiu, Kai-Wei Chang, Song-Chun Zhu, Oyvind Tafjord, Peter Clark, and Ashwin Kalyan. Learn to explain: Multimodal reasoning via thought chains for science question answering. In *The 36th Conference on Neural Information Processing Systems (NeurIPS)*, 2022. [7](#)
- [27] Mitch Marcus, Grace Kim, Mary Ann Marcinkiewicz, Robert MacIntyre, Ann Bies, Mark Ferguson, Karen Katz, and Britta Schasberger. The penn treebank: Annotating predicate argument structure. In *Human Language Technology: Proceedings of a Workshop held at Plainsboro, New Jersey, March 8-11, 1994*, 1994. [7](#)
- [28] Stephen Merity, Caiming Xiong, James Bradbury, and Richard Socher. Pointer sentinel mixture models. *arXiv preprint arXiv:1609.07843*, 2016. [7](#)

- [29] Adam Paszke, Sam Gross, Francisco Massa, Adam Lerer, James Bradbury, Gregory Chanan, Trevor Killeen, Zeming Lin, Natalia Gimelshein, Luca Antiga, et al. PyTorch: An imperative style, high-performance deep learning library. *Advances in neural information processing systems*, 32, 2019. 7
- [30] Alec Radford. Improving language understanding by generative pre-training. *Preprint*, 2018. 26
- [31] Colin Raffel, Noam Shazeer, Adam Roberts, Katherine Lee, Sharan Narang, Michael Matena, Yanqi Zhou, Wei Li, and Peter J Liu. Exploring the limits of transfer learning with a unified text-to-text transformer. *Journal of machine learning research*, 21(140):1–67, 2020. 7
- [32] Rajarshi Saha, Naomi Sagan, Varun Srivastava, Andrea Goldsmith, and Mert Pilanci. Compressing large language models using low rank and low precision decomposition. *Advances in Neural Information Processing Systems*, 37: 88981–89018, 2024. 1, 2
- [33] Tara N Sainath, Brian Kingsbury, Vikas Sindhwani, Ebru Arisoy, and Bhuvana Ramabhadran. Low-rank matrix factorization for deep neural network training with high-dimensional output targets. In *2013 IEEE international conference on acoustics, speech and signal processing*, pages 6655–6659. IEEE, 2013. 2, 3, 14
- [34] Utkarsh Saxena, Gobinda Saha, Sakshi Choudhary, and Kaushik Roy. Eigen attention: Attention in low-rank space for KV cache compression. *arXiv preprint arXiv:2408.05646*, 2024. 1, 2
- [35] Steffen Schotthöfer, Emanuele Zangrando, Jonas Kusch, Gianluca Ceruti, and Francesco Tudisco. Low-rank lottery tickets: finding efficient low-rank neural networks via matrix differential equations. *Advances in Neural Information Processing Systems*, 35:20051–20063, 2022. 1
- [36] Roy Schwartz, Jesse Dodge, Noah A Smith, and Oren Etzioni. Green AI. *Communications of the ACM*, 63(12):54–63, 2020. 1
- [37] Jianlin Su, Murtadha Ahmed, Yu Lu, Shengfeng Pan, Wen Bo, and Yunfeng Liu. RoFormer: Enhanced transformer with rotary position embedding. *Neurocomputing*, 568:127063, 2024. 27
- [38] Mingjie Sun, Zhuang Liu, Anna Bair, and J Zico Kolter. A simple and effective pruning approach for large language models. *arXiv preprint arXiv:2306.11695*, 2023. 1, 3, 7, 14, 33
- [39] Hugo Touvron, Louis Martin, Kevin Stone, Peter Albert, Amjad Almahairi, Yasmine Babaei, Nikolay Bashlykov, Soumya Batra, Prajjwal Bhargava, Shruti Bhosale, et al. Llama 2: Open foundation and fine-tuned chat models. *arXiv preprint arXiv:2307.09288*, 2023. 1
- [40] Changyuan Wang, Ziwei Wang, Xiuwei Xu, Yansong Tang, Jie Zhou, and Jiwen Lu. Q-VLM: Post-training quantization for large vision-language models. *arXiv preprint arXiv:2410.08119*, 2024. 1, 2
- [41] Xin Wang, Yu Zheng, Zhongwei Wan, and Mi Zhang. SVD-LLM: Truncation-aware singular value decomposition for large language model compression. *arXiv preprint arXiv:2403.07378*, 2024. 2
- [42] Jason Wei, Yi Tay, Rishi Bommasani, Colin Raffel, Barret Zoph, Sebastian Borgeaud, Dani Yogatama, Maarten Bosma, Denny Zhou, Donald Metzler, et al. Emergent abilities of large language models. *arXiv preprint arXiv:2206.07682*, 2022. 1
- [43] T Wolf. Huggingface’s transformers: State-of-the-art natural language processing. *arXiv preprint arXiv:1910.03771*, 2019. 7
- [44] Canwen Xu and Julian McAuley. A survey on model compression and acceleration for pretrained language models. In *Proceedings of the AAAI Conference on Artificial Intelligence*, pages 10566–10575, 2023. 1
- [45] Yibo Yang, Xiaojie Li, Zhongzhu Zhou, Shuaiwen Leon Song, Jianlong Wu, Liqiang Nie, and Bernard Ghanem. CorDA: Context-oriented decomposition adaptation of large language models. *arXiv preprint arXiv:2406.05223*, 2024. 3, 14
- [46] Zhewei Yao, Reza Yazdani Aminabadi, Minjia Zhang, Xiaoxia Wu, Conglong Li, and Yuxiong He. ZeroQuant: Efficient and affordable post-training quantization for large-scale transformers. *Advances in Neural Information Processing Systems*, 35:27168–27183, 2022. 7
- [47] Zhihang Yuan, Yuzhang Shang, Yue Song, Qiang Wu, Yan Yan, and Guangyu Sun. ASVD: Activation-aware singular value decomposition for compressing large language models. *arXiv preprint arXiv:2312.05821*, 2023. 1, 2, 3, 14
- [48] Zhihang Yuan, Yuzhang Shang, Yang Zhou, Zhen Dong, Zhe Zhou, Chenhao Xue, Bingzhe Wu, Zhikai Li, Qingyi Gu, Yong Jae Lee, et al. LLM inference unveiled: Survey and roofline model insights. *arXiv preprint arXiv:2402.16363*, 2024. 1
- [49] Susan Zhang, Stephen Roller, Naman Goyal, Mikel Artetxe, Moya Chen, Shuohui Chen, Christopher Dewan, Mona Diab, Xian Li, Xi Victoria Lin, et al. OPT: Open pre-trained transformer language models. *arXiv preprint arXiv:2205.01068*, 2022. 7, 35
- [50] Xunyu Zhu, Jian Li, Yong Liu, Can Ma, and Weiping Wang. A survey on model compression for large language models. *Transactions of the Association for Computational Linguistics*, 12:1556–1577, 2024. 1

## A. Weight-Aware Compression

### A.1. Plain SVD

Given a pretrained weight matrix  $W \in \mathbb{R}^{d' \times d}$ , we wish to approximate it with a low-rank structure:

$$\hat{W} = B \times A, \quad (23)$$

where  $\hat{W} \in \mathbb{R}^{d' \times d}$  is an approximated weight,  $B \in \mathbb{R}^{d' \times r}$  and  $A \in \mathbb{R}^{r \times d}$  are low-rank matrices with a rank  $r \leq d, d'$ . We assume  $d' \leq d$  for simplicity, as modifying for  $d' \geq d$  is straightforward.

Consider the approximation loss:

$$\mathcal{L} = \|W - \hat{W}\|^2 \quad (24)$$

$$= \|W - BA\|^2. \quad (25)$$

The best solution is given by SVD of  $W$  as follows:

$$A = J^+ V, \quad (26)$$

$$B = U S J, \quad (27)$$

where  $U \in \mathbb{R}^{d' \times r}$  is  $r$  most-principal left-singular vectors,  $S = \text{diag}[\sigma_1, \dots, \sigma_r] \in \mathbb{R}^{r \times r}$  is diagonal singular-values, and  $V \in \mathbb{R}^{r \times d}$  is the most-principal right-singular vectors for  $W$ :

$$U S V = \text{svd}_r[W], \quad (28)$$

where we assume the singular values are sorted in the descending order:  $\sigma_1 \geq \sigma_2 \geq \dots \geq \sigma_r$ . The loss is the accumulation of all the squared singular-values outside the rank  $r$ :  $\mathcal{L}_{\min} = \sum_{i>r} \sigma_i^2$ .

### A.2. Junction Matrix

There is no literature discussing the choice of a junction matrix  $J \in \mathbb{R}^{r \times r}$ , which has no impact on performance, provided that  $S J J^+ = S$  is satisfied. There are many suitable choices for this matrix  $J$ , such as:

- Left singular:  $J = I$ ;
- Right singular:  $J = S^+$ ;
- Symmetry singular:  $J = [S^{\frac{1}{2}}]^+$ .
- Left block identity:  $J = [U S]_{:,r}^+$
- Right block identity:  $J = [V]_{:,r}$

Although there is no performance impact by the choice of  $J$ , it is notable that the block identity which is based on block LU factorization can significantly reduce the number of parameters and FLOPs by  $r^2$ . This parameter reduction is particularly significant in high-dimensional (high-rank) latent cases. For example, when the weight is a size of  $d = d' = 2048$ , even with the half-rank latent  $r = d/2 = 1024$ , there is no parameter reduction as the dense compression and decompression matrices  $B$  takes  $2dr = d^2$  parameters. Hence, the 50% latent has no benefit in complexity but only for KV cache memory reduction as discussed in DeepSeek-V3 [24]. It is even worse for  $r > d/2$ : e.g., if we use 75% latent of  $r = 0.75d = 1536$ , the total parameter and FLOPs increases by 50% of the original weight (i.e.,  $2rd - d^2 = d^2/2$ ). However, using the block identity form, we can save  $r^2$ , and the total FLOPs will be always less than the original weight:  $2rd - r^2 < d^2$  for any  $r < d$ .

## B. Activation-Aware Compression

Consider an input token  $X \in \mathbb{R}^{d \times l}$  for a context length  $l \gg d$ , the linear projection output  $Y \in \mathbb{R}^{d' \times l}$  is:

$$Y = W X. \quad (29)$$

We assume that no bias is used for simplicity.

We wish to minimize the expected approximation error of output activation vectors between the true  $Y$  and the approximation  $\hat{Y} \in \mathbb{R}^{d' \times l}$ :

$$\hat{Y} = \hat{W} X, \quad (30)$$

projected by a low-rank weight  $\hat{W} = BA$ . Consider the loss function:

$$\mathcal{L} = \mathbb{E}_X \|Y - \hat{Y}\|^2 \quad (31)$$

$$= \mathbb{E}_X \|(W - \hat{W})X\|^2 \quad (32)$$

$$= \mathbb{E}_X \|(W - BA)X\|^2 \quad (33)$$

$$= \text{tr}[(W - BA)\mathbb{E}_X[XX^\top](W - BA)^\top] \quad (34)$$

$$= \text{tr}[(W - BA)C(W - BA)^\top] \quad (35)$$

$$= \|WC^{\frac{1}{2}} - BAC^{\frac{1}{2}}\|^2, \quad (36)$$

where  $C = \mathbb{E}_X[XX^\top] \in \mathbb{R}^{d \times d}$  is a (positive semidefinite) correlation matrix of the input vector.

The loss function of the activation-aware distillation in (36) is identical to the weight-aware distillation in (25) by transforming as:

$$W \rightarrow W' = WC^{\frac{1}{2}}, \quad (37)$$

$$A \rightarrow A' = AC^{\frac{1}{2}}. \quad (38)$$

Hence, the optimal solution is obtained similarly.

Specifically, from (26), (27), and (28), we have

$$A' = AC^{\frac{1}{2}} = J^+V', \quad (39)$$

$$B = U'S'J, \quad (40)$$

where  $U' \in \mathbb{R}^{d' \times d'}$ ,  $S' \in \mathbb{R}^{d' \times d}$ , and  $V' \in \mathbb{R}^{d \times d}$  are SVD of  $W' = WC^{\frac{1}{2}}$ :

$$U'S'V' = \text{svd}[WC^{\frac{1}{2}}]. \quad (41)$$

From (39), we finally obtain optimal  $A$  as:

$$A = J^+S'V'[C^{\frac{1}{2}}]^+. \quad (42)$$

## B.1. Pre-Conditioning Matrix

ASVD [47] proposed to use a projection matrix  $P \in \mathbb{R}^{d \times d}$  on weights before SVD:  $\text{svd}[WP]$ . The optimal projection  $P$  is apparently the square-root covariance  $P = C^{\frac{1}{2}}$ , while there are many other approximated projections that were considered in literature:

- Root-covariance:  $P = (XX^\top + \lambda I)^{\frac{1}{2}}$
- Covariance (e.g., CorDA [45]):  $P = XX^\top$
- Diagonal L2-norm (e.g., WandA [38]):  $P = \text{diag}[XX^\top]^{\frac{1}{2}}$
- Diagonal L1-norm (e.g., AWQ [23], ASVD [47]):  $P = \text{diag}[\|X\|_1, \dots, \|X\|_1]$
- Diagonal Hessian (e.g., OBS [12], GPTQ [11], SparseGPT [10]):  $P = \text{diag}[(XX^\top + \lambda I)^{-1}]^{\frac{1}{2}}$
- Identity (Plain SVD, e.g., [33]):  $P = I$

In the context of fine-tuning initialization, CorDA [45] uses covariance matrix  $C$  without square root, which should be worse than the square-root covariance. Fig. 7 demonstrates the benefit for random weights approximation with covariance drawn from the Wishart distribution. GPTQ [11] and SparseGPT [10] use another preconditioning matrix based on optimal brain surgeon (OBS) [12] using Hessian, in the context of quantization and pruning. Similarly, we can use it for low-rank compression as we have evaluated. In the context of pruning, WandA [38] proposed a simpler diagonal projection based on  $\ell_2$ -norm, while it achieves an excellent performance. AWQ and ASVD used the diagonal  $\ell_1$ -norm, while the theoretical justification is missing. They introduced another exponent factor to adjust.

## B.2. Bias Update

When the bias is there, we have

$$\mathcal{L} = \|(WX + b1^\top) - (BAX + \hat{b}1^\top)\|^2. \quad (43)$$



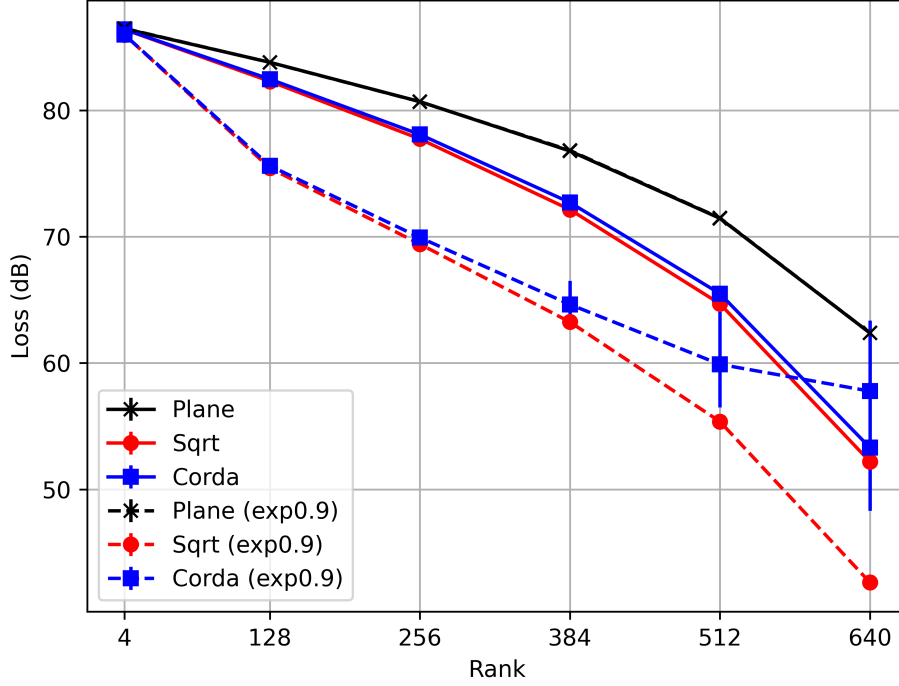


Figure 7. Comparison of SVD, CorDA, and RootCorDA.

The gradient with respect to  $\hat{b}$  is

$$\nabla \hat{b} = -2((WX + b1^\top) - (BAX + \hat{b}1^\top))1. \quad (44)$$

Hence, the optimal bias modification is:

$$\hat{b} = b + (W - BA)\mu, \quad (45)$$

where  $\mu = X1/1^\top 1 \in \mathbb{R}^{d \times 1}$  is a mean bias of input activation. Plugging into the loss, we have

$$\mathcal{L} = \|(W - BA)(X - \mu 1^\top)\|^2 \quad (46)$$

$$= \text{tr}[(W - BA) \underbrace{(X - \mu 1^\top)(X - \mu 1^\top)^\top}_{C_0 \in \mathbb{R}^{d \times d}} (W - BA)^\top] \quad (47)$$

$$= \|(W - BA)C_0^{\frac{1}{2}}\|^2. \quad (48)$$

Hence, the optimal solution is the SVD of weight multiplied with square root of covariance  $C_0$  not auto-correlation  $(XX^\top)$ :

$$C_0 = (C - \mu\mu^\top)l. \quad (49)$$

### C. Activation-Aware Joint QKV Compression

Consider minimizing QKV activation:

$$\mathcal{L} = \left\| \underbrace{\begin{bmatrix} W_q \\ W_k \\ W_v \end{bmatrix}}_{W \in \mathbb{R}^{3d' \times d}} X - \underbrace{\begin{bmatrix} B_q \\ B_k \\ B_v \end{bmatrix}}_{B \in \mathbb{R}^{3d' \times r}} AX \right\|^2. \quad (50)$$

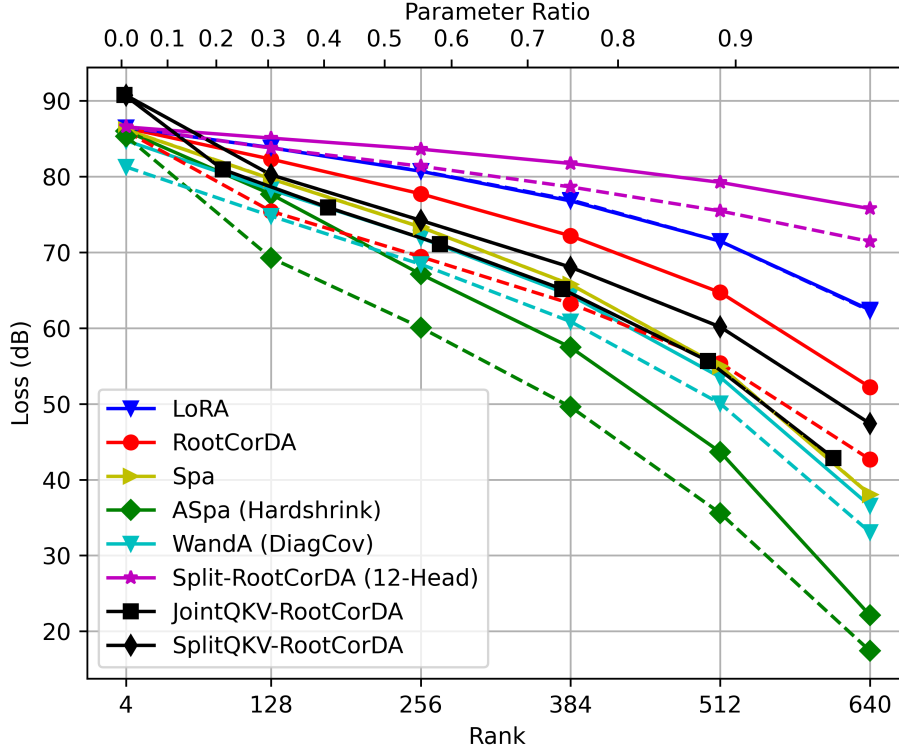


Figure 8. Joint-QKV vs split-QKV approximation.

In this case, the optimal solution is an SVD of  $WC^{\frac{1}{2}}$ .

Note that this is different from QKV individual optimization:

$$\mathcal{L}' = \sum_{i \in [q, k, v]} \|W_i X - B_i A_i X\|^2 \quad (51)$$

$$= \left\| \underbrace{\begin{bmatrix} W_q \\ W_k \\ W_v \end{bmatrix}}_{A \in \mathbb{R}^{3d' \times d}} X - \underbrace{\begin{bmatrix} B_q & O & O \\ O & B_k & O \\ O & O & B_v \end{bmatrix}}_{B \in \mathbb{R}^{3d' \times 3r}} \underbrace{\begin{bmatrix} A_q \\ A_k \\ A_v \end{bmatrix}}_{W \in \mathbb{R}^{3r \times d}} X \right\|^2. \quad (52)$$

The solution is 3 SVDs:  $W_i C^{\frac{1}{2}}$ .

The key difference: (i) the shared vs. non-shared compression matrix  $A$ ; (ii) block-diagonal vs. dense decomposition matrix  $B$ . The number of parameters will be  $r(3d' + d)$  from  $3r(d' + d)$ , allowing 50% more rank for joint QKV when  $d' = d$ . When we use LU factorization, the number of parameters will be  $r(3d' + d - r)$  from  $3r(d' + d - r)$ . We show the benefit of joint-QKV activation-aware distillation in Fig. 8.

Nevertheless, the relative magnitudes over Q/K/V are not well-treated for joint case, and it could be worse in the global performance in the end.

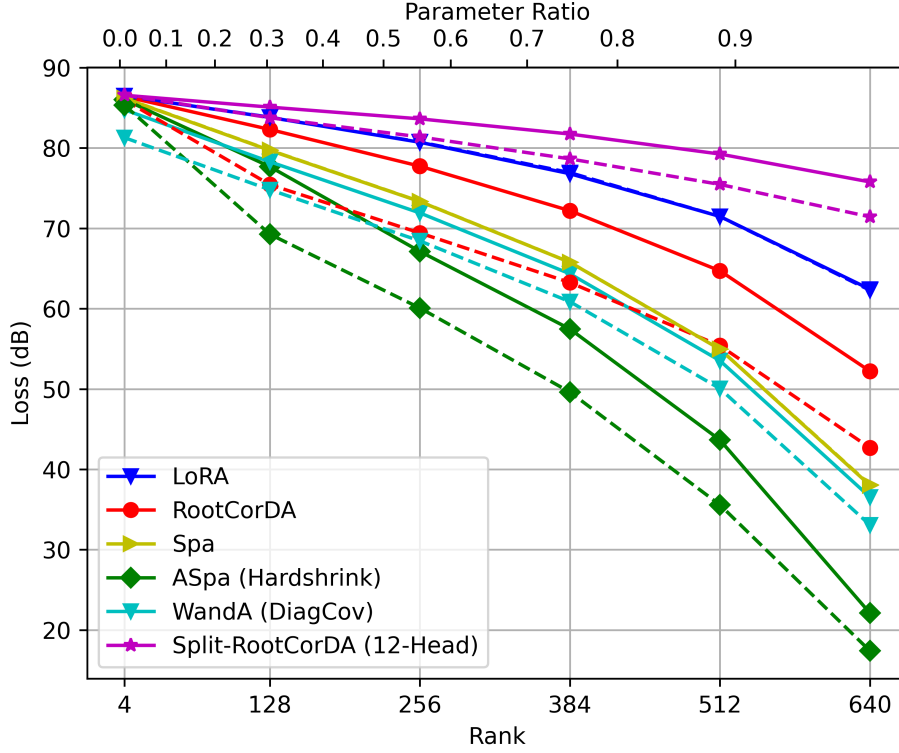


Figure 9. Split-head activation-aware approximation had terrible performance.

## D. Split-Head Compression

Typically, the weight matrix is split into multiple heads, what happens if we use split-head activation loss? Consider

$$\mathcal{L} = \sum_{i=1}^h \|W_i X - B_i A_i X\|^2 \quad (53)$$

$$= \left\| \underbrace{\begin{bmatrix} W_1 \\ \vdots \\ W_h \end{bmatrix}}_{W \in \mathbb{R}^{d' \times d}} X - \underbrace{\text{diag}[B_1, \dots, B_h]}_{B \in \mathbb{R}^{d' \times r}} \underbrace{\begin{bmatrix} A_1 \\ \vdots \\ A_h \end{bmatrix}}_{A \in \mathbb{R}^{r \times d}} X \right\|^2. \quad (54)$$

where  $W_i \in \mathbb{R}^{d'/h \times d}$ ,  $B_i \in \mathbb{R}^{d'/h \times r/h}$ ,  $A_i \in \mathbb{R}^{r/h \times d}$  are the  $i$ th head approximation with  $h$  being the number of heads. The solution is individual SVD of  $W_i C^{\frac{1}{2}}$ . However, as decomposition matrix  $B$  is sparse block diagonal, it is not efficient than joint head approximation. It is shown in Fig. 9.

## E. Multi-Head Attention (MHA)

Typically, the attention projection uses a square weight  $d' = d$ , but it is divided into multiple heads such that:

$$W_q = \begin{bmatrix} W_{q,1} \\ W_{q,2} \\ \vdots \\ W_{q,h} \end{bmatrix} \in \mathbb{R}^{d \times d}, \quad W_k = \begin{bmatrix} W_{k,1} \\ W_{k,2} \\ \vdots \\ W_{k,h} \end{bmatrix} \in \mathbb{R}^{d \times d}, \quad (55)$$

where  $W_{q,i} \in \mathbb{R}^{d/h \times d}$  and  $W_{k,i} \in \mathbb{R}^{d/h \times d}$  are the  $i$ th head projection weights, and  $h$  is number of heads. The analysis so far is still valid for per-head low-rank approximation to regard  $d' = d/h$ .

However, joint-head low-rank approximation may have a benefit over head-wise low-rank approximation. The  $i$ th head attention map is given as:

$$M_i = X^\top W_{q,i}^\top W_{k,i} X. \quad (56)$$

When we jointly decompose the low-rank with independent rank  $r_q$  and  $r_k$ :  $\hat{W}_q = B_q A_q$  and  $\hat{W}_k = B_k A_k$  for  $B_q, A_q^\top \in \mathbb{R}^{d \times r_q}$ ,  $B_k, A_k^\top \in \mathbb{R}^{d \times r_k}$ , we can write  $\hat{W}_{q,i} = B_{q,i} A_q$  and  $\hat{W}_{k,i} = B_{k,i} A_k$  for  $B_{q,i} \in \mathbb{R}^{d/h \times r_q}$  and  $B_{k,i} \in \mathbb{R}^{d/h \times r_k}$ , i.e., the compression matrix  $A$  is shared, and decompression matrix  $B$  is individual over multiple heads. It suggests that the rank  $r_q$  and  $r_k$  should not be lower than  $d/h$ , otherwise some heads can be redundant.

For arbitrary  $X$  (worst-case), we may consider minimizing

$$\mathcal{L} = \sum_{i=1}^h \left\| \underbrace{W_{q,i}^\top W_{k,i}}_{G_i \in \mathbb{R}^{d \times d}} - \underbrace{A_q^\top}_{H_i \in \mathbb{R}^{r_q \times r_k}} B_{q,i}^\top B_{k,i} A_k \right\|^2 \quad (57)$$

$$= \sum_{i=1}^h \|G_i - A_q^\top H_i A_k\|^2. \quad (58)$$

Note that  $G_i = W_{q,i}^\top W_{k,i} \in \mathbb{R}^{d \times d}$  is at most of rank  $d/h$ . And the rank of  $H_i = B_{q,i}^\top B_{k,i} \in \mathbb{R}^{r_q \times r_k}$  is not greater than  $r = \min(r_q, r_k, d/h)$ .

Note that there is no loss in generality to restrict that  $A_q$  and  $A_k$  are ortho-normal, i.e.,  $A_q A_q^\top = I_{r_q}$  and  $A_k A_k^\top = I_{r_k}$ , as a full matrix  $H_i$  can absorb any non-ortho-normal impact. Then, we have

$$\mathcal{L} = \sum_{i=1}^h \text{tr}[G_i G_i^\top + A_q^\top H_i \underbrace{A_k A_k^\top}_{I_{r_k}} H_i^\top A_q - A_q^\top H_i A_k G_i^\top - G_i A_k^\top H_i^\top A_q] \quad (59)$$

$$= \sum_{i=1}^h \|G_i\|^2 + \text{tr}[H_i H_i^\top \underbrace{A_q A_q^\top}_{I_{r_q}}] - \text{tr}[H_i A_k G_i^\top A_q^\top + A_q G_i A_k^\top H_i^\top] \quad (60)$$

$$= \sum_{i=1}^h \|G_i\|^2 + \|H_i\|^2 - 2\text{tr}[H_i A_k G_i^\top A_q^\top]. \quad (61)$$

The gradients:

$$\nabla_{H_i} \mathcal{L} = 2H_i - 2A_q G_i A_k^\top. \quad (62)$$

The KKT condition for  $H_i$  given  $A_q$  and  $A_k$  is thus:

$$H_i = A_q G_i A_k^\top \quad (63)$$

$$= A_q W_{q,i}^\top W_{k,i} A_k^\top. \quad (64)$$

Putting it back to the loss, we obtain:

$$\mathcal{L} = \sum_{i=1}^h \|G_i\|^2 + \|H_i\|^2 - 2\text{tr}[H_i A_k G_i^\top A_q^\top] \quad (65)$$

$$= \sum_i \|G_i\|^2 + \|A_q G_i A_k^\top\|^2 - 2\text{tr}[A_q G_i A_k^\top A_k G_i^\top A_q^\top] \quad (66)$$

$$= \sum_{i=1}^h \|G_i\|^2 + \|A_q G_i A_k^\top\|^2 - 2\|A_q G_i A_k^\top\|^2 \quad (67)$$

$$= \sum_{i=1}^h \|G_i\|^2 - \|A_q G_i A_k^\top\|^2. \quad (68)$$

Let's rewrite as

$$\mathcal{L} = \sum_i \|G_i\|^2 - \|(A_k \otimes A_q) \text{vec}[G_i]\|^2 \quad (69)$$

$$= \sum_i \|G_i\|^2 - \sum_i \|(A_k \otimes A_q) \text{vec}[G_i]\|^2 \quad (70)$$

$$= \sum_i \|G_i\|^2 - \|(A_k \otimes A_q) \underbrace{[\text{vec}[G_1], \text{vec}[G_2], \dots, \text{vec}[G_h]]}_{G \in \mathbb{R}^{d \times d \times h}}\|^2 \quad (71)$$

$$= \|G\|^2 - \|(A_k \otimes A_q)G\|^2 \quad (72)$$

$$= \|G\|^2 - \|(I_h \otimes A_k \otimes A_q) \text{vec}[G]\|^2. \quad (73)$$

This is the 3-mode tensor-rank decomposition problem involving the high-order SVD (HOSVD) for folding  $G$  into the size of  $d \times d \times h$ , but with a restriction that the first mode plane is identity (it may suggest that we may be able to improve by relaxing this constraint).

HOSVD has no simple solution, while alternating method works well in practice. Specifically, each tensor plane is alternately obtained by left singular of the unfolded tensor in different axis. Given  $A_k$ , the best  $A_q$  is the  $r_q$  left singular:

$$A_q^\top \leftarrow \text{LeftSingular}_{r_q}(\underbrace{[G_1 A_k^\top, G_2 A_k^\top, \dots, G_h A_k^\top]}_{\mathbb{R}^{d \times r_k h}}) \quad (74)$$

$$= \text{LeftSingular}_{r_q}(\sum_i G_i A_k^\top A_k G_i^\top). \quad (75)$$

The loss will be the residual accumulation of the eigenvalues beyond the rank  $r_q$ . Then given  $A_q$ , the best  $A_k$  is the  $r_k$  left singular:

$$A_k^\top \leftarrow \text{LeftSingular}_{r_k}(\underbrace{[G_1^\top A_q^\top, G_2^\top A_q^\top, \dots, G_h^\top A_q^\top]}_{\mathbb{R}^{d \times r_q h}}) \quad (76)$$

$$= \text{LeftSingular}_{r_k}(\sum_i G_i^\top A_q^\top A_q G_i). \quad (77)$$

The loss will be the residual accumulation of the eigenvalues beyond the rank  $r_k$ . Iterating the above often achieves a good solution. NOTE: singular vectors of  $\sum_i G_i G_i^\top$  and  $\sum_i G_i^\top G_i$  can be a good initialization of  $A_q$  and  $A_k$ .

NOTE: the non-uniform choice of ranks  $r_q$  and  $r_k$  can be optimized to minimize the loss, rather than using the same rank. It can be adaptively adjusted from the eigenvalue distributions.

Once we obtained the HOSVD solution for tensor planes  $A_q$  and  $A_k$ , the tensor core  $H_i \in \mathbb{R}^{r_q \times r_k}$  is generated by (64) as  $H_i = A_q G_i A_k^\top = A_q W_{q,i}^\top W_{k,i} A_k^\top$ . Given optimized  $H_i$ , any arbitrary  $B_{q,i}$  and  $B_{k,i}$  provides the same error as long as it holds:

$$H_i = B_{q,i}^\top B_{k,i}. \quad (78)$$

The solution is

$$B_{q,i} = J_i^\top W_{q,i} A_q^\top, \quad (79)$$

$$B_{k,i} = J_i^\top W_{k,i} A_k^\top, \quad (80)$$

where  $J_i \in \mathbb{R}^{d/h \times d/h}$  is any arbitrary full-rank matrix of our choice. The most natural choice is identity:  $J_i = I_{d/h}$ .

Nevertheless, another simple solution will be

$$B_{q,i} = I_{d/h \times r_q}, \quad (81)$$

$$B_{k,i} = \begin{bmatrix} H_i \\ O_{(d/h - r_q) \times r_k} \end{bmatrix}, \quad (82)$$



when  $r_q \leq d/h$ . This has a benefit that query decompression does not require any memory and key decompression is a block sparse.

Another solution will be

$$B_{q,i} = \begin{bmatrix} H_i^\top \\ O_{(d/h-r_k) \times r_q} \end{bmatrix}, \quad (83)$$

$$B_{k,i} = I_{d/h \times r_k}, \quad (84)$$

when  $r_k \leq d/h$ . Similar benefit, but probably removing the requirement of query decompression is more beneficial than key decompression in practice.

When  $r_k, r_q \geq d/h$  (in most case?), we can select  $J_i$  such that  $B_{q,i}$  or  $B_{k,i}$  is block matrix to save  $(d/h)^2$  parameters from  $(r_q + r_k)d/h$ . For this case, fine-tuning two decompression  $B_{q,i}$  and  $B_{k,i}$  rather than a product  $H_i$  will be more parameter-efficient.

### E.1. Activation-Aware Multi-Head Latent Attention

Consider the loss:

$$\mathcal{L} = \sum_i \|M_i - \hat{M}_i\|^2 \quad (85)$$

$$= \sum_i \|X^\top \underbrace{(G_i - A_q^\top H_i A_k)}_{\Delta_i \in \mathbb{R}^{d \times d}} X\|^2 \quad (86)$$

$$= \sum_i \text{tr}[X^\top \Delta_i X X^\top \Delta_i^\top X] \quad (87)$$

$$= \sum_i \text{tr}[\Delta_i \underbrace{X X^\top}_{C \in \mathbb{R}^{d \times d}} \Delta_i^\top X X^\top] \quad (88)$$

$$= \sum_i \text{tr}[\Delta_i C \Delta_i^\top C] \quad (89)$$

$$= \sum_i \text{tr}[\Delta_i C^{\frac{1}{2}} C^{\frac{1}{2}} \Delta_i^\top C^{\frac{1}{2}} C^{\frac{1}{2}}] \quad (90)$$

$$= \sum_i \|C^{\frac{1}{2}} \Delta_i C^{\frac{1}{2}}\|^2 \quad (91)$$

$$= \sum_i \left\| \underbrace{C^{\frac{1}{2}} G_i C^{\frac{1}{2}}}_{G'_i} - \underbrace{C^{\frac{1}{2}} A_q^\top}_{A_q'^\top} H_i \underbrace{A_k C^{\frac{1}{2}}}_{A'_k} \right\|^2, \quad (92)$$

where  $C$  is a positive semi-definite of rank no greater than  $\min(d, l)$ .

In fact, the solution is same as the case without  $X$  comparing (58) and (92), where we can regard as

$$G_i \rightarrow G'_i = C^{\frac{1}{2}} G_i C^{\frac{1}{2}}, \quad (93)$$

$$A_q \rightarrow A'_q = A_q C^{\frac{1}{2}}, \quad (94)$$

$$A_k \rightarrow A'_k = A_k C^{\frac{1}{2}}. \quad (95)$$

Here, we can consider  $A_q C^{\frac{1}{2}}$  and  $A_k C^{\frac{1}{2}}$  are instead orthogonal, and thus the solution can be given by HOSVD likewise.

Fig. 10 shows the comparison between adaptive and non-adaptive distillation with activation/attention-aware methods.

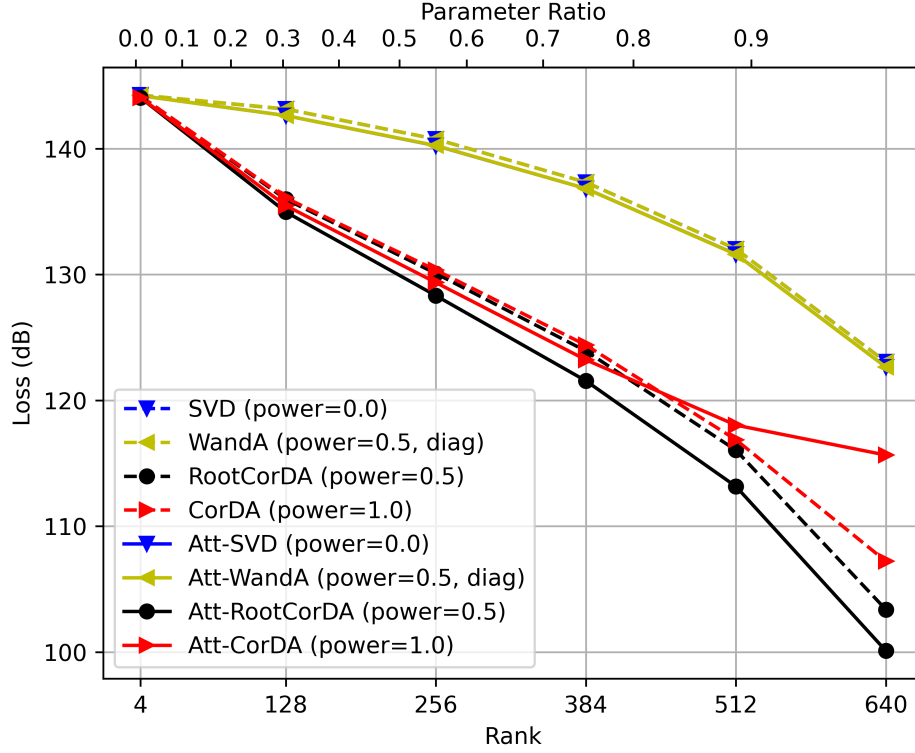


Figure 10. Attention-Aware vs. Activation-Aware Approximation. Loss is attention map error. Random query/key projections with Wishart sample correlation (0.9 decaying). WandA uses diagonal correlation.

## E.2. Bias Update

Some LLMs use bias for QKV. For this case, we need to modify the bias term as well. We have

$$\mathcal{L} = \sum_i \|(W_{q,i}X + b_{q,i}1^\top)^\top (W_{k,i}X + b_{k,i}1^\top) - (\hat{W}_{q,i}X + \hat{b}_{q,i}1^\top)^\top (\hat{W}_{k,i}X + \hat{b}_{k,i}1^\top)\|^2 \quad (96)$$

$$= \sum_i \left\| \left( \underbrace{\begin{bmatrix} W_{q,i} & b_{q,i} \end{bmatrix}}_{W'_{q,i} \in \mathbb{R}^{d/h \times (d+1)}} \underbrace{\begin{bmatrix} X \\ 1^\top \end{bmatrix}}_{X' \in \mathbb{R}^{(d+1) \times l}} \right)^\top \left( \underbrace{\begin{bmatrix} W_{k,i} & b_{k,i} \end{bmatrix}}_{W'_{k,i} \in \mathbb{R}^{d/h \times (d+1)}} \underbrace{\begin{bmatrix} X \\ 1^\top \end{bmatrix}}_{X' \in \mathbb{R}^{(d+1) \times l}} \right) - \left( \underbrace{\begin{bmatrix} \hat{W}_{q,i} & \hat{b}_{q,i} \end{bmatrix}}_{\hat{W}'_{q,i} \in \mathbb{R}^{d/h \times (d+1)}} \underbrace{\begin{bmatrix} X \\ 1^\top \end{bmatrix}}_{X' \in \mathbb{R}^{(d+1) \times l}} \right)^\top \left( \underbrace{\begin{bmatrix} \hat{W}_{k,i} & \hat{b}_{k,i} \end{bmatrix}}_{\hat{W}'_{k,i} \in \mathbb{R}^{d/h \times (d+1)}} \underbrace{\begin{bmatrix} X \\ 1^\top \end{bmatrix}}_{X' \in \mathbb{R}^{(d+1) \times l}} \right) \right\|^2 \quad (97)$$

$$= \sum_i \|X'^\top (W_{q,i}'^\top W_{k,i}' - \hat{W}_{q,i}'^\top \hat{W}_{k,i}')X'\|^2 \quad (98)$$

$$= \sum_i \|\tilde{C}^{\frac{1}{2}} (W_{q,i}'^\top W_{k,i}' - \hat{W}_{q,i}'^\top \hat{W}_{k,i}') \tilde{C}^{\frac{1}{2}}\|^2 \quad (99)$$

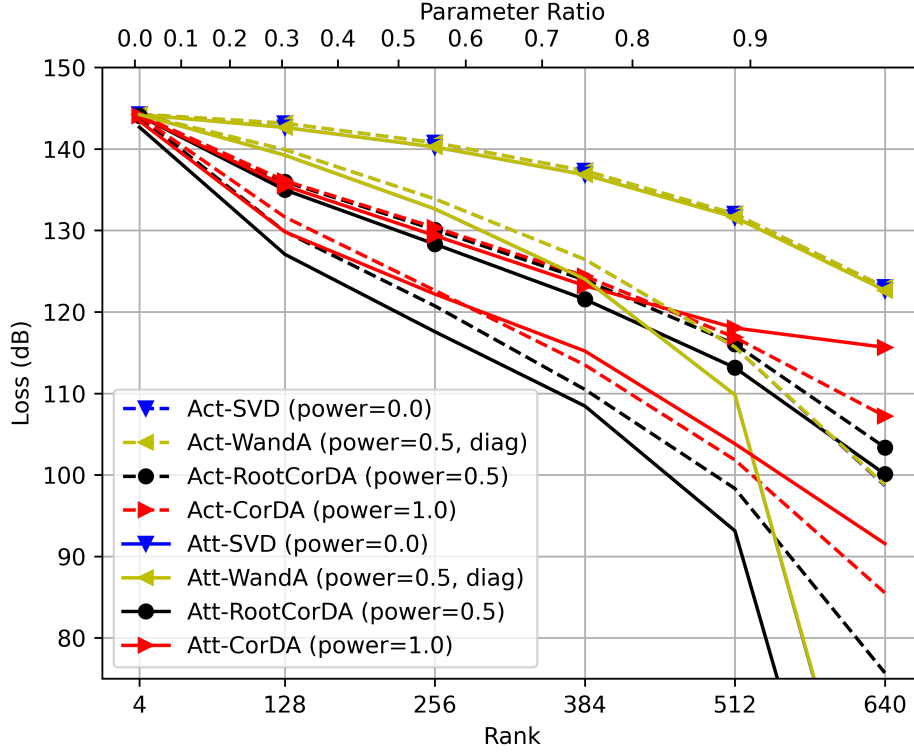


Figure 11. Sparse approximation for Attention-Aware vs. Activation-Aware distillation. No markers are sparse approximation. Sparse is better than low-rank.

where we have a modified covariance:

$$\tilde{C} = X'X'^\top \in \mathbb{R}^{(d+1) \times (d+1)} \quad (100)$$

$$= \begin{bmatrix} X \\ 1^\top \end{bmatrix} \begin{bmatrix} X^\top & 1 \end{bmatrix} \quad (101)$$

$$= \begin{bmatrix} lC & l\mu \\ l\mu^\top & l \end{bmatrix} = l \begin{bmatrix} C & \mu \\ \mu^\top & 1 \end{bmatrix} \quad (102)$$

$$= l \begin{bmatrix} C^{\frac{1}{2}} & O \\ \mu^\top C^{\frac{-1}{2}} & (1 - \mu^\top C^+ \mu)^{\frac{1}{2}} \end{bmatrix} \begin{bmatrix} C^{\frac{1}{2}} & C^{\frac{-1}{2}} \mu \\ O & (1 - \mu^\top C^+ \mu)^{\frac{1}{2}} \end{bmatrix} \quad (103)$$

where we assume  $C$  is normalized as  $C = XX^\top/l$ , and  $\mu \in \mathbb{R}^{d \times 1}$  is a mean of input tokens:  $\mu = X1/l$ . Then, we can omit  $l$ . Similar format but it cannot be solved by the same way as we have a structured low-rank expression:

$$\hat{W}'_{q,i}{}^\top \hat{W}'_{k,i} = \begin{bmatrix} A_q^\top & B_{q,i}^\top \\ \hat{b}_{q,i}^\top & \end{bmatrix} \begin{bmatrix} B_{k,i} A_k & \hat{b}_{k,i} \end{bmatrix} \quad (104)$$

$$= \underbrace{\begin{bmatrix} A_q^\top & O_{d \times 1} \\ O_{1 \times r_q} & 1 \end{bmatrix}}_{A_q'^\top \in \mathbb{R}^{(d+1) \times (r_q+1)}} \underbrace{\begin{bmatrix} B_{q,i}^\top \\ \hat{b}_{q,i}^\top \end{bmatrix}}_{B_{q,i}'^\top \in \mathbb{R}^{(r_q+1) \times d}} \underbrace{\begin{bmatrix} B_{k,i} & \hat{b}_{k,i} \end{bmatrix}}_{B_{k,i}' \in \mathbb{R}^{d \times (r_k+1)}} \underbrace{\begin{bmatrix} A_k & O_{r_k \times 1} \\ O_{1 \times d} & 1 \end{bmatrix}}_{A_k' \in \mathbb{R}^{(r_k+1) \times (d+1)}}. \quad (105)$$

We may use the HOSVD to decompose with one more rank for bias, while the compression matrix  $A'_q$  and  $A'_k$  needs to be a particular format. Nonetheless, we can modify the bias by the KKT condition:

$$A'_q \tilde{C} G_i \tilde{C} A'_k{}^\top = A'_q \tilde{C} A'_q{}^\top H'_i A'_k \tilde{C} A'_k{}^\top. \quad (106)$$

Hence we have

$$H'_i = (A'_q \tilde{C} A'_q{}^\top)^+ A'_q \tilde{C} G_i \tilde{C} A'_k{}^\top (A'_k \tilde{C} A'_k{}^\top)^+ \quad (107)$$

$$= \underbrace{(A'_q \tilde{C} A'_q{}^\top)^+ A'_q \tilde{C} W'_{q,i}{}^\top}_{B_{q,i}^\top} \underbrace{W'_{k,i} \tilde{C} A'_k{}^\top (A'_k \tilde{C} A'_k{}^\top)^+}_{B_{k,i}}. \quad (108)$$

Thus, given optimized  $A_q$  and  $A_k$ , we have optimized decomposition matrix with updated bias:

$$B'_{q,i} = [B_{q,i} \quad \hat{b}_{q,i}] \quad (109)$$

$$= J_i^\top W'_{q,i} \tilde{C} A'_q{}^\top (A'_q \tilde{C} A'_q{}^\top)^+ \quad (110)$$

$$= J_i^\top [W_{q,i} \quad b_{q,i}] \tilde{C} A'_q{}^\top (A'_q \tilde{C} A'_q{}^\top)^+ \quad (111)$$

$$= J_i^\top [W_{q,i} \quad b_{q,i}] \begin{bmatrix} C A_q^\top & \mu \\ \mu^\top A_q^\top & 1 \end{bmatrix} \begin{bmatrix} A_q C A_q^\top & A_q \mu \\ \mu^\top A_q^\top & 1 \end{bmatrix}^+ \quad (112)$$

$$= J_i^\top [W_{q,i} \quad b_{q,i}] \begin{bmatrix} C A_q^\top & \mu \\ \mu^\top A_q^\top & 1 \end{bmatrix} \begin{bmatrix} I & O \\ -\mu^\top A_q^\top & 1 \end{bmatrix} \begin{bmatrix} (A_q C A_q^\top - A_q \mu \mu^\top A_q^\top)^+ & O \\ O & 1 \end{bmatrix} \begin{bmatrix} I & -A_q \mu \\ O & 1 \end{bmatrix} \quad (113)$$

$$= J_i^\top [W_{q,i} \quad b_{q,i}] \begin{bmatrix} (C - \mu \mu^\top) A_q^\top (A_q C A_q^\top - A_q \mu \mu^\top A_q^\top)^+ & -(C - \mu \mu^\top) A_q^\top (A_q C A_q^\top - A_q \mu \mu^\top A_q^\top)^+ A_q \mu + \mu \\ O & 1 \end{bmatrix} \quad (114)$$

$$= J_i^\top [W_{q,i} (C - \mu \mu^\top) A_q^\top (A_q C A_q^\top - A_q \mu \mu^\top A_q^\top)^+ \quad -W_{q,i} (C - \mu \mu^\top) A_q^\top (A_q C A_q^\top - A_q \mu \mu^\top A_q^\top)^+ A_q \mu + W_{q,i} \mu + b_{q,i}]. \quad (115)$$

It gives the bias modifications:

$$\hat{b}_q = \text{diag}[J_i] (b_q + W_q \mu - W_q (C - \mu \mu^\top) A_q^\top (A_q C A_q^\top - A_q \mu \mu^\top A_q^\top)^+ A_q \mu), \quad (116)$$

$$\hat{b}_k = \text{diag}[J_i^+] (b_k + W_k \mu - W_k (C - \mu \mu^\top) A_k^\top (A_k C A_k^\top - A_k \mu \mu^\top A_k^\top)^+ A_k \mu). \quad (117)$$

We define the centered auto-correlation:

$$C_0 = C - \mu \mu^\top. \quad (118)$$

Then, we assume that the optimal compression matrices  $A_q$  and  $A_k$  are orthogonal on  $C_0^{\frac{1}{2}}$ :

$$A_q C_0 A_q^\top = I_{r_q}, \quad (119)$$

$$A_k C_0 A_k^\top = I_{r_k}. \quad (120)$$

In this case, the bias modification can reduce to

$$\hat{b}_q = \text{diag}[J_i] (b_q + W_q \mu - W_q C_0 A_q^\top A_q \mu), \quad (121)$$

$$\hat{b}_k = \text{diag}[J_i^+] (b_k + W_k \mu - W_k C_0 A_k^\top A_k \mu). \quad (122)$$

For this case, we have

$$A'_q \tilde{C} A_q^\top = \begin{bmatrix} A_q C A_q^\top & A_q \mu \\ \mu^\top A_q^\top & 1 \end{bmatrix}, \quad (123)$$

$$(A'_q \tilde{C} A_q^\top)^+ = \begin{bmatrix} I & -A_q \mu \\ -\mu^\top A_q^\top & 1 + \mu^\top A_q^\top A_q \mu \end{bmatrix}, \quad (124)$$

$$A'_q (A'_q \tilde{C} A_q^\top)^+ A_q^\top = \begin{bmatrix} A_q^\top A_q & -A_q^\top A_q \mu \\ -\mu^\top A_q^\top A_q & 1 + \mu^\top A_q^\top A_q \mu \end{bmatrix}, \quad (125)$$

$$A'_q (A'_q \tilde{C} A_q^\top)^+ A_q^\top \tilde{C} = \begin{bmatrix} A_q^\top A_q C_0 & O \\ \mu^\top - \mu^\top A_q^\top A_q C_0 & 1 \end{bmatrix}, \quad (126)$$

$$\tilde{C} A'_q (A'_q \tilde{C} A_q^\top)^+ A_q^\top = \begin{bmatrix} C_0 A_q^\top A_q & \mu - C_0 A_q^\top A_q \mu \\ O & 1 \end{bmatrix}, \quad (127)$$

$$\tilde{C} A'_q (A'_q \tilde{C} A_q^\top)^+ A_q^\top \tilde{C} = \begin{bmatrix} C_0 A_q^\top A_q C_0 + \mu \mu^\top & \mu \\ \mu^\top & 1 \end{bmatrix}. \quad (128)$$

Plugging the optimized  $H_i$ , the loss is expressed as

$$\mathcal{L} = \sum_i \left\| \tilde{C}^{\frac{1}{2}} W_{q,i}'^\top W_{k,i}' \tilde{C}^{\frac{1}{2}} - \tilde{C}^{\frac{1}{2}} A_q^\top (A'_q \tilde{C} A_q^\top)^+ A'_q \tilde{C} W_{q,i}'^\top W_{k,i}' \tilde{C} A_k^\top (A'_k \tilde{C} A_k^\top)^+ A'_k \tilde{C}^{\frac{1}{2}} \right\|^2 \quad (129)$$

$$= \sum_i \left\| \tilde{C}^{\frac{1}{2}} W_{q,i}'^\top W_{k,i}' \tilde{C}^{\frac{1}{2}} \right\|^2 - \left\| \tilde{C}^{\frac{1}{2}} A_q^\top H_i A_k \tilde{C}^{\frac{1}{2}} \right\|^2 \quad (130)$$

$$= \sum_i \left\| \tilde{C}^{\frac{1}{2}} W_{q,i}'^\top W_{k,i}' \tilde{C}^{\frac{1}{2}} \right\|^2 - \left\| \tilde{C}^{\frac{1}{2}} A_q^\top (A'_q \tilde{C} A_q^\top)^+ A'_q \tilde{C} W_{q,i}'^\top W_{k,i}' \tilde{C} A_k^\top (A'_k \tilde{C} A_k^\top)^+ A'_k \tilde{C}^{\frac{1}{2}} \right\|^2 \quad (131)$$

$$= \sum_i \left\| \tilde{C}^{\frac{1}{2}} W_{q,i}'^\top W_{k,i}' \tilde{C}^{\frac{1}{2}} \right\|^2 - \text{tr}[\tilde{C} A_q^\top (A'_q \tilde{C} A_q^\top)^+ A'_q \tilde{C} \underbrace{W_{q,i}'^\top W_{k,i}' \tilde{C} A_k^\top (A'_k \tilde{C} A_k^\top)^+ A'_k \tilde{C} W_{k,i}'^\top W_{q,i}'}_{G_{q,i} \in \mathbb{R}^{(d+1) \times (d+1)}}]. \quad (132)$$

$$= \sum_i \left\| \tilde{C}^{\frac{1}{2}} W_{q,i}'^\top W_{k,i}' \tilde{C}^{\frac{1}{2}} \right\|^2 - \text{tr}[\tilde{C} A_q^\top (A'_q \tilde{C} A_q^\top)^+ A'_q \tilde{C} \underbrace{W_{q,i}'^\top W_{k,i}' \tilde{C} A_k^\top (A'_k \tilde{C} A_k^\top)^+ A'_k \tilde{C} W_{k,i}'^\top W_{q,i}'}_{G_{q,i} \in \mathbb{R}^{(d+1) \times (d+1)}}]. \quad (133)$$

Focusing on optimizing  $A_q$ , the second term will be

$$\sum_i \text{tr} \left[ \left( \begin{bmatrix} C_0 A_q^\top A_q C_0 & O \\ O & 0 \end{bmatrix} + \begin{bmatrix} \mu \\ 1 \end{bmatrix} \begin{bmatrix} \mu \\ 1 \end{bmatrix}^\top \right) G_{q,i} \right] = \sum_i \text{tr} \left[ \begin{bmatrix} C_0 A_q^\top A_q C_0 & O \\ O & 0 \end{bmatrix} G_{q,i} \right] + \text{c.c.} \quad (134)$$

$$= \text{tr} \left[ C_0 A_q^\top A_q C_0 I_{d \times (d+1)} \sum_i G_{q,i} I_{(d+1) \times d} \right] + \text{c.c.} \quad (135)$$

$$= \|A_q C_0 (I_{d \times (d+1)} \sum_i G_{q,i} I_{(d+1) \times d})^{\frac{1}{2}}\|^2 + \text{c.c.} \quad (136)$$

Hence the optimal  $A_q$  is the right-singular vectors:

$$A_q C_0^{\frac{1}{2}} = \text{RightSingular}_{r_q} \left[ C_0^{\frac{1}{2}} I_{d \times (d+1)} \left( \sum_i G_{q,i} \right) I_{(d+1) \times d} C_0^{\frac{1}{2}} \right]. \quad (137)$$

In fact, we can re-write  $G_{q,i}$  as

$$G_{q,i} = \begin{bmatrix} W_{q,i}^\top \\ b_{q,i}^\top \end{bmatrix} \begin{bmatrix} W_{k,i} & b_{k,i} \end{bmatrix} \left( \begin{bmatrix} C_0 A_k^\top A_k C_0 & O \\ O & 0 \end{bmatrix} + \begin{bmatrix} \mu \\ 1 \end{bmatrix} \begin{bmatrix} \mu \\ 1 \end{bmatrix}^\top \right) \begin{bmatrix} W_{k,i}^\top \\ b_{k,i}^\top \end{bmatrix} \begin{bmatrix} W_{q,i} & b_{q,i} \end{bmatrix} \quad (138)$$

$$= \begin{bmatrix} W_{q,i}^\top \\ b_{q,i}^\top \end{bmatrix} \left( W_{k,i} C_0 A_k^\top A_k C_0 W_{k,i}^\top + (W_{k,i} \mu + b_{k,i})(W_{k,i} \mu + b_{k,i})^\top \right) \begin{bmatrix} W_{q,i} & b_{q,i} \end{bmatrix}. \quad (139)$$

Hence, we have

$$A_q C_0^{\frac{1}{2}} = \text{RightSingular}_{r_k} \left[ \sum_i C_0^{\frac{1}{2}} W_{q,i}^\top W_{k,i} C_0 A_k^\top A_k C_0 W_{k,i}^\top W_{q,i} C_0^{\frac{1}{2}} + \sum_i C_0^{\frac{1}{2}} W_{q,i}^\top (W_{k,i} \mu + b_{k,i})(W_{k,i} \mu + b_{k,i})^\top W_{q,i} C_0^{\frac{1}{2}} \right]. \quad (140)$$



The first term is the solution if no bias and mean are present.

Similarly the solution for  $A_k$  is given by

$$A_k C_0^{\frac{1}{2}} = \text{RightSingular}_{r_k} [C_0^{\frac{1}{2}} I_{d \times (d+1)} (\sum_i G_{k,i}) I_{(d+1) \times d} C_0^{\frac{1}{2}}] \quad (141)$$

$$\begin{aligned} &= \text{RightSingular}_{r_q} \left[ \sum_i C_0^{\frac{1}{2}} W_{k,i}^\top W_{q,i} C_0 A_q^\top A_q C_0 W_{q,i}^\top W_{k,i} C_0^{\frac{1}{2}} \right. \\ &\quad \left. + \sum_i C_0^{\frac{1}{2}} W_{k,i}^\top (W_{q,i} \mu + b_{q,i}) (W_{q,i} \mu + b_{q,i})^\top W_{k,i} C_0^{\frac{1}{2}} \right]. \end{aligned} \quad (142)$$

where

$$G_{k,i} = W_{k,i}^\top W'_{q,i} \tilde{C} A_q'^\top (A_q' \tilde{C} A_q'^\top)^+ A_q' \tilde{C} W_{q,i}' W_{k,i}' \quad (143)$$

$$= \begin{bmatrix} W_{k,i}^\top \\ b_{k,i}^\top \end{bmatrix} W_{q,i} C_0 A_q^\top A_q C_0 W_{q,i}^\top \begin{bmatrix} W_{k,i} & b_{k,i} \end{bmatrix} + \begin{bmatrix} W_{k,i}^\top \\ b_{k,i}^\top \end{bmatrix} (W_{q,i} \mu + b_{q,i}) (W_{q,i} \mu + b_{q,i})^\top \begin{bmatrix} W_{k,i} & b_{k,i} \end{bmatrix}. \quad (144)$$

### E.3. Grouped Query Attention (GQA)

MHA (e.g., for Llama-2) uses  $h$ -heads for query, key, and value. However, Llama-3 uses grouped query attention (GQA), where the number of heads for key and value are smaller than the number of heads for query. Let  $n_q$  be the query group size. Then, the number of query heads is  $n_q h$ , whereas  $h$  is the number of KV heads. Suppose  $n_q$  is the integer so that simple repetition can be used. Q and K projections:

$$W_q = \begin{bmatrix} W_{q,1} \\ W_{q,2} \\ \vdots \\ W_{q,n_q h} \end{bmatrix} \in \mathbb{R}^{n_q h d' \times d}, \quad W_k = \begin{bmatrix} W_{k,1} \\ W_{k,2} \\ \vdots \\ W_{k,h} \end{bmatrix} \in \mathbb{R}^{h d' \times d}, \quad (145)$$

for  $W_{q,i} \in \mathbb{R}^{d' \times d}$ ,  $W_{k,i} \in \mathbb{R}^{d' \times d}$  with the head dimension  $d'$ . Llama-3 uses repeat-interleave to match the number of heads by repeating the KV projections  $n_q$ -times:

$$W'_k = \begin{bmatrix} W_{k,1} \\ W_{k,1} \\ \vdots \\ W_{k,1} \\ \vdots \\ W_{k,h} \end{bmatrix} \in \mathbb{R}^{n_q h d' \times d}. \quad (146)$$

For such GQA, we have attention map for the  $j$ th head in the  $i$ th group ( $j \in \mathbb{Z}_h^+$ ,  $i \in \mathbb{Z}_{n_q}^+$ ):

$$M_{i,j} = X^\top W_{q,i,j}^\top W_{k,i,j} X, \quad (147)$$

where we use an index convention:  $W_{q,i,j} = W_{q, i n_q + j}$ .

Consider the loss:

$$\mathcal{L} = \sum_{i,j} \|M_{i,j} - \hat{M}_{i,j}\|^2 \quad (148)$$

$$= \sum_{i,j} \|X^\top \underbrace{(W_{q,i,j}^\top W_{k,i,j} - A_q^\top \overbrace{B_{q,i,j}^\top B_{k,i,j}}^{H_{i,j} \in \mathbb{R}^{r_q \times r_k}} A_k)}_{\Delta_{i,j} \in \mathbb{R}^{d \times d}} X\|^2 \quad (149)$$

$$= \sum_{i,j} \|C^{\frac{1}{2}} G_{i,j} C^{\frac{1}{2}} - C^{\frac{1}{2}} A_q^\top H_{i,j} A_k C^{\frac{1}{2}}\|^2. \quad (150)$$

Hence the solution can be obtained with HOSVD likewise MHA in Sec. E.1.

## F. Positional Encoding

### F.1. Additive PE

Consider additive PE for a token  $X \in \mathbb{R}^{d \times l}$ :

$$X' = X + E, \quad (151)$$

where  $E \in \mathbb{R}^{d \times l}$  is a positional embedding matrix. Often it is sinusoidal like

$$E_{i,j} = \exp(j2\pi f_i j/l), \quad (152)$$

with a predefined frequency  $f_i$  for  $i \in \mathbb{Z}_d$ . Note that complex rotation is not used in typical case, and instead split into  $\cos$  and  $\sin$ . Many work also considered trainable PE [17, 30].

In this additive PE case, the solution is same by replacing the correlation matrix  $C$  with

$$C' = \mathbb{E}_X[X'X'^\top] \quad (153)$$

$$= \mathbb{E}_X[(X + E)(X + E)^\top] \quad (154)$$

$$= C + EE^\top + \mathbb{E}_X[XE^\top + EX^\top]. \quad (155)$$

For zero-mean token case, it reduces to  $C + EE^\top$ . For static token case, we may use  $(X + E)(X + E)^\top$  directly.

Nevertheless, some PE methods [6] use different additive PE for query and key individually:

$$X_q = X + E_q, \quad (156)$$

$$X_k = X + E_k. \quad (157)$$

In this case, the attention map will have bias terms:

$$M_i = X_q^\top W_{q,i}^\top W_{k,i} X_k \quad (158)$$

$$= X^\top G_i X + X^\top G_i E_k + E_q^\top G_i X + E_q^\top G_i E_k. \quad (159)$$

There are many variants to relax them or generalize them.

Consider loss:

$$\mathcal{L} = \sum_i \|X_q^\top \Delta_i X_k\|^2 \quad (160)$$

$$= \sum_i \text{tr}[\Delta_i \underbrace{X_k X_k^\top}_{C_k \in \mathbb{R}^{d \times d}} \Delta_i^\top \underbrace{X_q X_q^\top}_{C_q \in \mathbb{R}^{d \times d}}] \quad (161)$$

$$= \sum_i \text{tr}[\Delta_i C_k \Delta_i^\top C_q] \quad (162)$$

$$= \sum_i \text{tr}[\Delta_i C_k^{\frac{1}{2}} C_k^{\frac{1}{2}} \Delta_i^\top C_q^{\frac{1}{2}} C_q^{\frac{1}{2}}] \quad (163)$$

$$= \sum_i \text{tr}[C_q^{\frac{1}{2}} \Delta_i C_k^{\frac{1}{2}} C_k^{\frac{1}{2}} \Delta_i^\top C_q^{\frac{1}{2}}] \quad (164)$$

$$= \sum_i \|C_q^{\frac{1}{2}} \Delta_i C_k^{\frac{1}{2}}\|^2 \quad (165)$$

$$= \sum_i \left\| \underbrace{C_q^{\frac{1}{2}} G_i C_k^{\frac{1}{2}}}_{G'_i} - \underbrace{C_q^{\frac{1}{2}} A_q^\top}_{A_q'^\top} \underbrace{H_i A_k C_k^{\frac{1}{2}}}_{A'_k} \right\|^2. \quad (166)$$

Hence, we can still solve it with HOSVD.

## F.2. Concatenative PE

Another PE uses concatenation:

$$Q_i = \begin{bmatrix} W_{q,i}X \\ E_{q,i} \end{bmatrix}, \quad (167)$$

$$K_i = \begin{bmatrix} W_{k,i}X \\ E_{k,i} \end{bmatrix}. \quad (168)$$

Then, the attention map will be

$$M_i = Q_i^\top K_i \quad (169)$$

$$= X^\top G_i X + E_{q,i}^\top E_{k,i}, \quad (170)$$

which has just a bias term  $E_q^\top E_k$  and there is no impact in loss function with low-rank approximation.

## F.3. Multiplicative PE

Consider a multiplicative PE for token  $X$ :

$$X' = X \odot E, \quad (171)$$

where  $\odot$  denotes Hadamard product. We just need to replace the correlation with  $C' = X'X'^\top$  to solve in a straightforward manner.

However, rotary PE (RoPE) [37] uses multiplicative PE on query and key, not token  $X$ . More precisely, we can represent per token:

$$q_{i,m} = \Theta_{i,m} W_{q,i} x_m, \quad (172)$$

$$k_{i,m} = \Theta_{i,m} W_{k,i} x_m, \quad (173)$$

where  $\Theta_{i,m}$  is a block diagonal rotation matrix for  $i$ th head and  $m$ th token, such that  $\Theta_{i,m}^\top \Theta_{i,n} = \Theta_{i,n-m}$ .

For example, Llama-2 uses the same RoPE for all heads with block rotation:

$$\Theta_{i,m} = \begin{bmatrix} \cos(m\Phi) & -\sin(m\Phi) \\ \sin(m\Phi) & \cos(m\Phi) \end{bmatrix} \in \mathbb{R}^{d/h \times d/h}, \quad (174)$$

$$\Phi = \text{diag}[\{\theta^{-2ih/d}\}_{i=0}^{d/2h-1}] \in \mathbb{R}^{d/2h \times d/2h}, \quad (175)$$

with a base rope theta of  $\theta = 10^4$ .

We have the loss:

$$\mathcal{L} = \mathbb{E}_X \sum_{i,m,n} \|q_{i,m}^\top k_{i,m} - \hat{q}_{i,m}^\top \hat{k}_{i,m}\|^2 \quad (176)$$

$$= \mathbb{E}_X \sum_{i,m,n} \|x_m^\top \underbrace{(W_{q,i}^\top \Theta_{i,n-m} W_{k,i} - A_q^\top B_{q,i}^\top \Theta_{i,n-m} B_{k,i} A_k)}_{\Delta_{i,n-m} \in \mathbb{R}^{d \times d}} x_n\|^2 \quad (177)$$

$$= \mathbb{E}_X \sum_{i,m,n} \text{tr}[\Delta_{i,n-m} x_n x_n^\top \Delta_{i,n-m}^\top x_m x_m^\top] \quad (178)$$

$$= \sum_{i,m,n} \text{tr}[\Delta_{i,n-m} C \Delta_{i,n-m}^\top C] \quad (179)$$

$$= \sum_{i,m,n} \|C^{\frac{1}{2}} \Delta_{i,n-m} C^{\frac{1}{2}}\|^2 \quad (180)$$

$$= \sum_{i,m,n} \left\| \underbrace{C^{\frac{1}{2}} W_{q,i}^\top \Theta_{i,n-m} W_{k,i} C^{\frac{1}{2}}}_{W'_{i,n-m}} - \underbrace{C^{\frac{1}{2}} A_q^\top}_{A_q'^\top} \underbrace{B_{q,i}^\top \Theta_{i,n-m} B_{k,i}}_{H_{i,n-m}} \underbrace{A_k C^{\frac{1}{2}}}_{A'_k} \right\|^2 \quad (181)$$

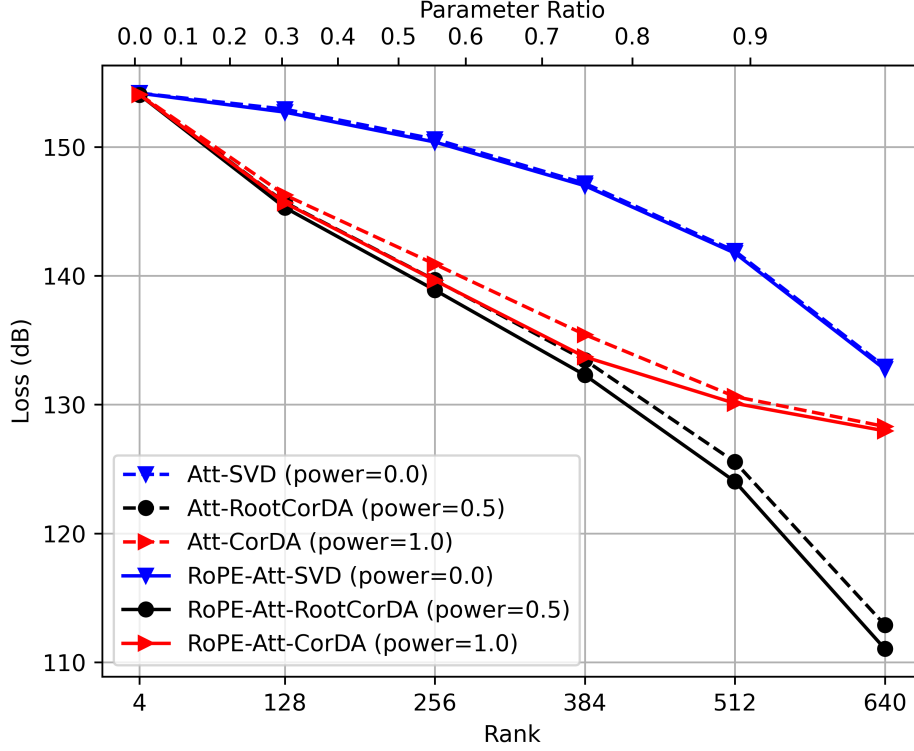


Figure 12. RoPE-Attention-Aware Distillation: 10-token window.

where we assumed  $x_m$  and  $x_n$  are independent. Then, we can solve it with HOSVD. However, considering all token lengths over  $m$  and  $n$  is not practical, and we may need to consider attention windows such as  $|n - m| \leq 5$  to optimize. When a causal mask is used, we do not need to sum over  $m > n$  but only  $m \geq n$ .

NOTE: we can generalize RoPE with other unitary rotations.

Fig. 12 shows the result of HOSVD with/without RoPE consideration. The loss is calculated over 10-token window, with RoPE base theta of  $10^4$ , used in Llama-2, while the hidden size is still 768. HOSVD without RoPE consideration was already a good approximation as it is optimal at diagonal token. RoPE-aware HOSVD offers additional 1–2 dB gain.

## G. Joint Value-Output Compression

Many LLMs have output projection after QKV attention. The attention output will be

$$Y = \sum_i W_{o,i} W_{v,i} X \sigma(M_i^\top), \quad (182)$$

where  $W_{o,i} \in \mathbb{R}^{d \times d/h}$  is the  $i$ th head output projection, and  $Y \in \mathbb{R}^{d \times l}$  is the attention output. This motivates us to optimize value projection and output projection jointly.

NOTE:  $W_{o,i} W_{v,i}$  can be triangularized by LU factorization to save the number of parameters from  $2d^2$  to  $2d^2 - d^2/h$  without any performance loss.

As  $\sigma(M_i)$  is just weighting  $X$ , we may assume that the statistics still holds as  $\mathbb{E}[X \sigma(M_i) \sigma(M_i)^\top X^\top] = C$  for uncorrelated tokens. Hence, we end up with optimizing

$$\mathcal{L} = \|W_o W_v C^{\frac{1}{2}} - B_o \underbrace{A_o B_v}_H A_v C^{\frac{1}{2}}\|^2. \quad (183)$$

Hence, both projections can be combined together.

Nevertheless, when we consider minimizing individual head projection loss for arbitrary attention weights:

$$\mathcal{L} = \sum_i \left\| \underbrace{W_{o,i} W_{v,i} C^{\frac{1}{2}}}_{G_i \in \mathbb{R}^{d \times d}} - B_o \underbrace{A_{o,i} B_{v,i}}_{H_i \in \mathbb{R}^{r_o \times r_v}} \underbrace{A_v C^{\frac{1}{2}}}_{A'_v} \right\|^2. \quad (184)$$

Then the solution is HOSVD:

$$B_o = \text{RightSingular}_{r_o} \left[ \sum_i G_i A_v'^{\top} A_v' G_i^{\top} \right], \quad (185)$$

$$A_v' = \text{RightSingular}_{r_v} \left[ \sum_i G_i^{\top} B_o B_o^{\top} G_i \right], \quad (186)$$

$$A_{o,i} = B_o^{\top} W_{o,i} J_i \quad (187)$$

$$B_{v,i} = J_i^+ W_{v,i} A_v'^{\top}, \quad (188)$$

for arbitrary full-rank matrix  $J_i \in \mathbb{R}^{d/h \times d/h}$ . Selecting  $J_i$  can save the number of parameters by up to  $d/h \times d/h$ .

### G.1. Bias Update

Some LLMs such as OPT uses bias in QKVO. Let's consider bias impact. The attention output will be:

$$Y = \sum_i W_{o,i} (W_{v,i} X + b_{v,i} \mathbf{1}^{\top}) \sigma(M_i) + b_{o,i} \mathbf{1}^{\top} \quad (189)$$

$$= \sum_i W_{o,i} W_{v,i} X \sigma(M_i) + W_{o,i} b_{v,i} \mathbf{1}^{\top} \sigma(M_i) + b_{o,i} \mathbf{1}^{\top}. \quad (190)$$

Considering any arbitrary attention map  $M_i$ , we may want to optimize:

$$\mathcal{L} = \sum_i \|W_{o,i} (W_{v,i} X + b_{v,i} \mathbf{1}^{\top}) + b_{o,i} \mathbf{1}^{\top} - \hat{W}_{o,i} (\hat{W}_{v,i} X + \hat{b}_{v,i} \mathbf{1}^{\top}) - \hat{b}_{o,i} \mathbf{1}^{\top}\|^2. \quad (191)$$

The gradient with respect to  $\hat{b}_o$  is given

$$-(W_{o,i} (W_{v,i} X + b_{v,i} \mathbf{1}^{\top}) + b_{o,i} \mathbf{1}^{\top} - \hat{W}_{o,i} (\hat{W}_{v,i} X + \hat{b}_{v,i} \mathbf{1}^{\top}) - \hat{b}_{o,i} \mathbf{1}^{\top}) \mathbf{1}. \quad (192)$$

Thus the KKT condition gives:

$$\hat{b}_{o,i} = b_{o,i} + W_{o,i} (W_{v,i} \mu + b_{v,i}) - \hat{W}_{o,i} (\hat{W}_{v,i} \mu + \hat{b}_{v,i}). \quad (193)$$

Plugging into the loss gives:

$$\mathcal{L} = \sum_i \|W_{o,i} W_{v,i} (X - \mu \mathbf{1}^{\top}) - \hat{W}_{o,i} \hat{W}_{v,i} (X - \mu \mathbf{1}^{\top})\|^2 \quad (194)$$

$$= \sum_i \left\| \underbrace{W_{o,i} W_{v,i} C_0^{\frac{1}{2}}}_{G_i \in \mathbb{R}^{d \times d}} - B_o \underbrace{A_{o,i} B_{v,i}}_{H_i \in \mathbb{R}^{r_o \times r_v}} A_v C_0^{\frac{1}{2}} \right\|^2. \quad (195)$$

Here,  $C_0 = (X - \mu \mathbf{1}^{\top})(X - \mu \mathbf{1}^{\top})^{\top}$  is centered covariance (it can be normalized). Hence, this is solved by HOSVD:

$$B_o = \text{RightSingular}_{r_o} \left[ \sum_i G_i C_0 A_v^{\top} A_v C_0 G_i^{\top} \right], \quad (196)$$

$$A_v C_0^{\frac{1}{2}} = \text{RightSingular}_{r_o} \left[ \sum_i C_0^{\frac{1}{2}} G_i^{\top} B_o B_o^{\top} G_i C_0^{\frac{1}{2}} \right]. \quad (197)$$

Note that  $\hat{b}_v$  has no impact as it can be absorbed by  $\hat{b}_o$ . Hence, we can keep the original bias or changed to zero bias.

## G.2. Attention-Aware Joint VO Compression

The output projection module takes the input token:

$$X_{o,i} = W_{v,i} X \sigma(M_i^\top). \quad (198)$$

The covariance of the token is

$$C_{o,i} = X_{o,i} X_{o,i}^\top \quad (199)$$

$$= W_{v,i} X \sigma(M_i^\top) \sigma(M_i) W_{v,i}^\top. \quad (200)$$

Over the heads, we have cross-correlation terms:

$$X_o = \begin{bmatrix} W_{v,1} X \sigma(M_1^\top) \\ W_{v,2} X \sigma(M_2^\top) \\ \vdots \\ W_{v,h} X \sigma(M_h^\top) \end{bmatrix} \quad (201)$$

$$= \underbrace{\text{diag}[W_{v,1}, W_{v,2}, \dots, W_{v,h}]}_{W'_v \in \mathbb{R}^{hd_h \times hd_h}} (I_h \otimes X) \underbrace{\begin{bmatrix} \sigma(M_1^\top) \\ \sigma(M_2^\top) \\ \vdots \\ \sigma(M_h^\top) \end{bmatrix}}_{X' \in \mathbb{R}^{hd \times l}}. \quad (202)$$

We consider using the covariance of output projection module not value projection module instead. The covariance of the output projection  $C_o \in \mathbb{R}^{hd_h \times hd_h}$  is given as

$$C_o = X_o X_o^\top \quad (203)$$

$$= W'_v \underbrace{X' X'^\top}_{C_v \in \mathbb{R}^{hd \times hd}} W_v'^\top. \quad (204)$$

Using this attention-aware token statistics  $C_v$  can be more accurate to optimize, rather than simple token statistics  $C$ .

The value projection module takes the input token  $X$  typically. However, there is no impact when we instead take the attention-weighted token for each head before value projection:  $X'$ . Even though we have no statistics on this, we can predict it from  $C_o$  as  $C_o = W'_v C_v W_v'^\top$ :

$$C_v = W_v'^+ C_o [W_v'^+]^\top. \quad (205)$$

Note that this is at most the rank of  $hd_h$ .

The loss will be

$$\mathcal{L} = \left\| \sum_i W_{o,i} W_{v,i} X \sigma(M_i^\top) - \hat{W}_{o,i} \hat{W}_{v,i} X \sigma(M_i^\top) \right\|^2 \quad (206)$$

$$= \|W_o W_v' X' - \hat{W}_o \hat{W}_v' X'\|^2 \quad (207)$$

$$= \|W_o W_v' C_v^{\frac{1}{2}} - \hat{W}_o \hat{W}_v' C_v^{\frac{1}{2}}\|^2 \quad (208)$$

$$= \|W_o C_o^{\frac{1}{2}} - \hat{W}_o \hat{W}_v' W_v'^+ C_o^{\frac{1}{2}}\|^2. \quad (209)$$

Here we have

$$\hat{W}_v' W_v'^+ = \text{diag}[\hat{W}_{v,1} W_{v,1}^\top (W_{v,1} W_{v,1}^\top)^+, \hat{W}_{v,2} W_{v,2}^\top (W_{v,2} W_{v,2}^\top)^+, \dots, \hat{W}_{v,h} W_{v,h}^\top (W_{v,h} W_{v,h}^\top)^+] \in \mathbb{R}^{hd_h \times hd_h}. \quad (210)$$

We write:

$$\mathcal{L} = \left\| \sum_i W_{o,i} [C_o^{\frac{1}{2}}]_i - B_o \underbrace{A_{o,i} B_{v,i}}_{H_i \in \mathbb{R}^{r_o \times r_v}} A_v W_{v,i}^+ [C_0^{\frac{1}{2}}]_i \right\|^2 \quad (211)$$

$$= \left\| W_o C_o^{\frac{1}{2}} - B_o \sum_i H_i A_v W_{v,i}^+ [C_0^{\frac{1}{2}}]_i \right\|^2 \quad (212)$$

$$= \left\| W_o C_o^{\frac{1}{2}} - B_o \underbrace{\begin{bmatrix} H_1 & \dots & H_h \end{bmatrix}}_{H \in \mathbb{R}^{r_o \times h r_v}} (I_h \otimes A_v) \text{diag}[W_{v,1}^+, \dots, W_{v,h}^+] C_0^{\frac{1}{2}} \right\|^2. \quad (213)$$

Note that  $H_i$  is of rank up to  $\min(r_o, r_v, d_h)$ .

Gradient:

$$\nabla_H \mathcal{L} = - \left( B_o \right)^\top \left( W_o C_o^{\frac{1}{2}} - B_o H (I_h \otimes A_v) W_v'^+ C_0^{\frac{1}{2}} \right) \left( (I_h \otimes A_v) W_v'^+ C_0^{\frac{1}{2}} \right)^\top, \quad (214)$$

$$\nabla_{A_{o,j}} \mathcal{L} = - \left( B_o \right)^\top \left( W_o C_o^{\frac{1}{2}} - B_o H (I_h \otimes A_v) W_v'^+ C_0^{\frac{1}{2}} \right) \left( B_{v,j} A_v W_{v,j}^+ [C_0^{\frac{1}{2}}]_j \right)^\top, \quad (215)$$

$$\nabla_{B_{v,j}} \mathcal{L} = - \left( B_o A_{o,j} \right)^\top \left( W_o C_o^{\frac{1}{2}} - B_o H (I_h \otimes A_v) W_v'^+ C_0^{\frac{1}{2}} \right) \left( A_v W_{v,j}^+ [C_0^{\frac{1}{2}}]_j \right)^\top, \quad (216)$$

$$\nabla_{B_o} \mathcal{L} = - \left( W_o C_o^{\frac{1}{2}} - B_o H (I_h \otimes A_v) W_v'^+ C_0^{\frac{1}{2}} \right) \left( H (I_h \otimes A_v) W_v'^+ C_0^{\frac{1}{2}} \right)^\top, \quad (217)$$

$$\nabla_{A_v} \mathcal{L} = - \sum_j \left( B_o H_j \right)^\top \left( W_o C_o^{\frac{1}{2}} - B_o \sum_i H_i A_v W_{v,i}^+ [C_0^{\frac{1}{2}}]_i \right) \left( W_{v,j}^+ [C_0^{\frac{1}{2}}]_j \right)^\top. \quad (218)$$

The optimal  $B_o$  is the left-singular of  $W_o C_o^{\frac{1}{2}}$ , having unitary condition:  $B_o^\top B_o = I_{r_o}$ .

From the first KKT, we have a linear system to solve for  $H$ :

$$H \begin{bmatrix} A_v W_{v,1}^+ [C_0^{\frac{1}{2}}]_1 \\ \vdots \\ A_v W_{v,h}^+ [C_0^{\frac{1}{2}}]_h \end{bmatrix} \begin{bmatrix} A_v W_{v,1}^+ [C_0^{\frac{1}{2}}]_1 \\ \vdots \\ A_v W_{v,h}^+ [C_0^{\frac{1}{2}}]_h \end{bmatrix}^\top = B_o^\top W_o C_o^{\frac{1}{2}} \begin{bmatrix} A_v W_{v,1}^+ [C_0^{\frac{1}{2}}]_1 \\ \vdots \\ A_v W_{v,h}^+ [C_0^{\frac{1}{2}}]_h \end{bmatrix}^\top. \quad (219)$$

Hence, we have

$$H = B_o^\top W_o C_o [W_v'^+]^\top (I_h \otimes A_v^\top) \left( (I_h \otimes A_v) W_v'^+ C_o [W_v'^+]^\top (I_h \otimes A_v^\top) \right)^\dagger. \quad (220)$$

Plugging into the loss, we have

$$\mathcal{L} = \|W_o C_o^{\frac{1}{2}}\|^2 - \left\| B_o^\top W_o C_o [W_v'^+]^\top (I_h \otimes A_v)^\top \left( (I_h \otimes A_v) W_v'^+ C_o [W_v'^+]^\top (I_h \otimes A_v)^\top \right)^{-\frac{1}{2}} \right\|^2 \quad (221)$$

The last KKT condition requires solving in vectorization:

$$\sum_{i,j} (G_j G_i^\top \otimes H_j^\top H_i) \text{vec}[A_v] = \sum_j \text{vec}[H_j B_o^\top W_o C_o^{\frac{1}{2}} G_j^\top], \quad (222)$$

where  $G_i \in \mathbb{R}^{d \times h d_h}$  is defined:

$$G_i = W_{v,i}^+ [C_0^{\frac{1}{2}}]_i. \quad (223)$$

## H. MLP-Aware Joint Compression

SparseLLM [3] proposed the way to sparsify MLP layer in LLM models as it consumes two thirds of trainable parameters. The key idea is to minimize the MLP loss, not local loss. LLM uses typically 2-layer MLP:

$$z = W_1 x + b_1, \quad (224)$$

$$a = \sigma(z), \quad (225)$$

$$y = W_2 a + b_2. \quad (226)$$



The first linear layer typically upsamples by a factor of four, and then the second linear layer downsamples to the same dimension. Activation-aware low-rank approximation can minimize loss individually for  $z$  given  $x$  and  $y$  given  $a$ , but not the MLP output  $y$  given  $x$ .

SparseLLM uses the closed-form solution to minimize:

$$\mathcal{L} = \alpha \|W_1 x + b_1 - z\|^2 + \beta \|a - \sigma(z)\|^2 + \gamma \|W_2 a + b_2 - y\|^2, \quad (227)$$

for auxiliary variables  $a$  and  $z$ , given pre-trained input  $x$  and output  $y$ .

Optimizing  $a$  can be obtained by ridge regression:

$$a^* = (\gamma W_2^\top W_2 + \beta I)^+ (\beta \sigma(z) + \gamma W_2^\top (y - b_2)). \quad (228)$$

Optimal  $z$  can be also obtained closed-form way with case for ReLU:

$$z_- = W_1 x + b_1, \quad (229)$$

$$z_+ = \frac{1}{\alpha + \beta} (\alpha z_- + \beta a), \quad (230)$$

depending on  $[z]_i$ 's sign.

The same approach can be used for low-rank approximation. Given  $z$ , we can optimize low-rank matrix  $\hat{W}_1 = B_1 A_1$  by SVD of  $(z - b_1)x^+ C_x^{\frac{1}{2}}$ , where  $(z - b_1)x^+ = (z - b_1)x^\top C_x^+$  corresponds to the effective weight matrix to map  $x$  onto  $z$ . Given  $a$ , we approximate  $\hat{W}_2 = B_2 A_2$  by SVD of  $(y - b_2)a^+ C_a^{\frac{1}{2}} = (y - b_2)a^\top C_a^{\frac{-1}{2}}$ , given correlation  $C_a = aa^\top$ .

## I. Sparse Matrix

Consider low-rank plus sparse decomposition:

$$\hat{W} = BA + D, \quad (231)$$

where  $D \in \mathbb{R}^{d' \times d}$  is a sparse matrix such that  $\|D\|_0 \leq \kappa$ . As discussed so far, given a  $D$  matrix, the best low-rank matrices are SVD of  $(W - D)C^{\frac{1}{2}}$ . Given  $BA$ , finding sparse  $D$  is an NP-hard problem, and often it is solved by greedy or relaxed methods such as matching pursuit and proximal gradient. Considering the  $\ell_1$  relaxation, we have

$$\mathcal{L}' = \|(D + BA - W)C^{\frac{1}{2}}\|^2 + \lambda(\|D\|_1 - \kappa). \quad (232)$$

Fast iterative shrinkage-threshold algorithm (FISTA) uses iterations with Nesterov's accelerating technique:

$$D_k = \mathcal{T}_{\lambda \mu_k} [D_{k-1} - 2\mu_k(D_{k-1} + BA - W)C], \quad (233)$$

$$\mu_{k+1} = \frac{1}{2}(1 + \sqrt{1 + 4\mu_k^2}), \quad (234)$$

$$D_k \leftarrow D_k + \frac{\mu_k - 1}{\mu_{k+1}}(D_k - D_{k-1}), \quad (235)$$

for iterations  $k = 1, 2, \dots$  with a stepsize  $\mu_1 = 1$ .  $\mathcal{T}_\alpha$  is a soft shrinkage operator:

$$\mathcal{T}_\alpha[x] = \text{sign}[x](x - \alpha)_+. \quad (236)$$

We may iterate SVD and FISTA. The choice of  $\lambda$  is crucial to have a target sparsity. It is not easy to adjust  $\lambda$  such that the target sparsity is achieved beforehand.

Alternatively, we use a regular gradient method with straight-through estimator (STE):

$$D = \underbrace{D - D.\text{detach}}_{\text{STE Trick}} + \mathcal{S}_\kappa[D.\text{detach}], \quad (237)$$

where  $\mathcal{S}_\kappa[\cdot]$  is a hard shrinkage operator, i.e., sparsification operator passing only  $\kappa$  elements having largest magnitude. This STE method has a benefit over FISTA: i) the sparsity can be specified; ii) any other loss function including the final

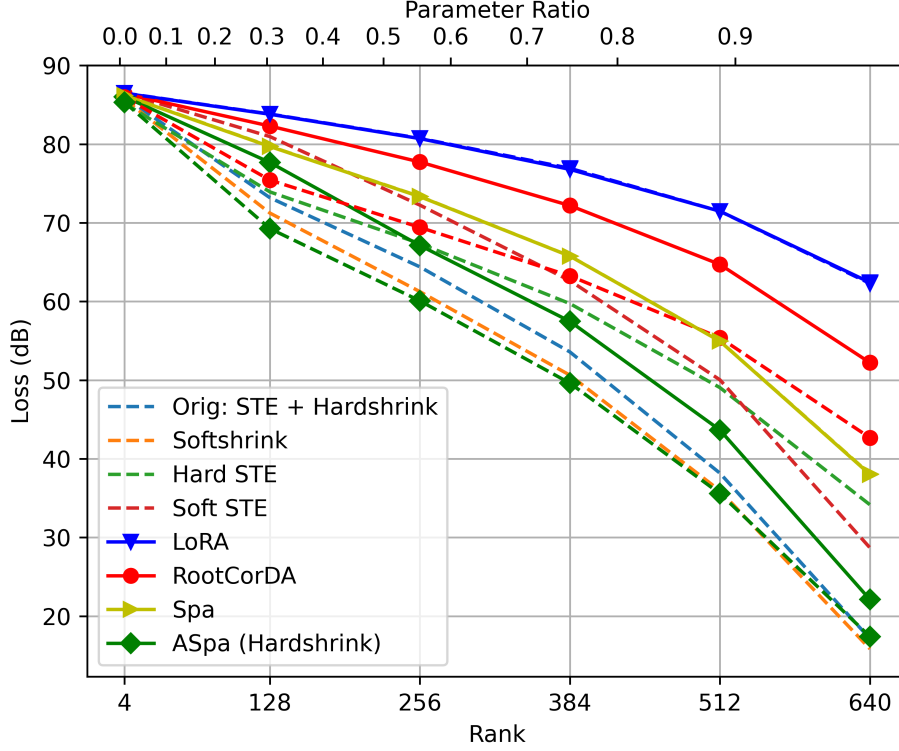


Figure 13. Random weight approximation with/without correlation. Correlation is sampled from Wishart distribution with covariance of identity or off-diagonal decaying of 0.9 factor. Weight is normal distributed.

downstream task loss can be incorporated; and iii) the quantization-aware training can be readily integrated in the STE projection. Nevertheless, soft shrink and hard shrink are actually differentiable, and we may not need to use STE. Fig. 13 shows the comparison of STE and Hard/Softshrink. In this experiment, Hardshrink works best.

We also notice that sparse approximation can be better than low-rank approximation. And, also joint low-rank plus sparse approximation did not work well as shown in Fig. 14.

However, unstructured sparse matrix may require index storage to memorize the non-zero entry locations. When we use a mask, it requires  $d'd$  binary memory as well as non-zero values in  $D$ . When the sparsity is small, keeping index will be more efficient, i.e., keeping  $\log_2(dd')\tau$ . Fig. 15 shows the case with sparsification for low-rank adapter  $B$ ,  $A$ , starting RootCorDA of rank 640 and 512. Although sparsified low-rank approximation has a benefit, it does not outperform sparse approximation alone.

Another possibility using sparse approximation is to sparsify LoRA matrices  $B$  and  $A$ . However, doing so may be poor because the product of two sparse matrices can be much more sparse: e.g., 50% sparse  $B$  and  $A$  will result in 25% sparse  $BA$ . Hence, using sparse matrices for  $B$  and  $A$  may be a bad solution. Similarly, using sparse  $W_q$  and  $W_k$  may be a poor combination for attention map approximation.

WandA [38], SparseGPT [10] and SparseLLM [3] use non-iterative solutions by considering only diagonal covariance:

$$C \rightarrow C \odot I_d. \quad (238)$$

This does not require iterative compressed sensing. However, the diagonal approximation has a degraded performance as in Fig. 16.

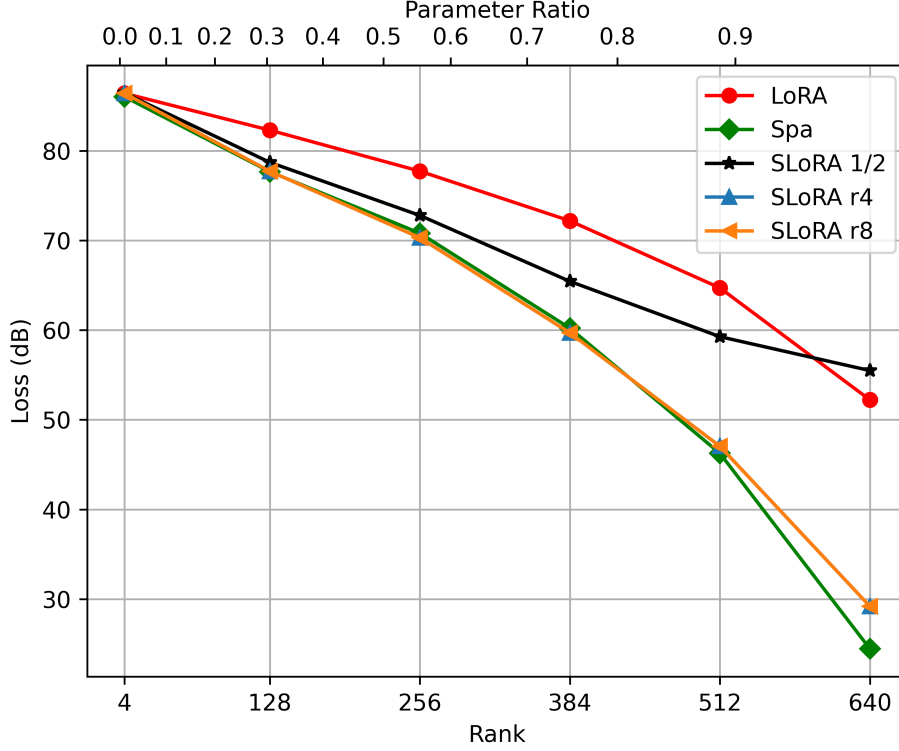


Figure 14. Low-rank plus sparse approximation does not outperform sparse-alone approximation.

### I.1. Quantization-Aware Distillation

We can use STE for quantization-aware distillation in a straightforward manner. Whatever the loss, we can use STE for the trainable parameters, e.g., for  $B$  and  $A$  low-rank matrices:

$$B \leftarrow B - B.\text{detach} + \mathcal{Q}[B.\text{detach}], \quad (239)$$

$$A \leftarrow A - A.\text{detach} + \mathcal{Q}[A.\text{detach}], \quad (240)$$

where we may consider a simple chunk-wise  $q$ -bit uniform quantization:

$$x' = \mathcal{Q}[x] \quad (241)$$

$$= \text{round}\left[(x - x_{\min}) \cdot \frac{2^q - 1}{x_{\max} - x_{\min}}\right] \cdot \frac{x_{\max} - x_{\min}}{2^q - 1} + x_{\min}, \quad (242)$$

where  $x_{\min}$  and  $x_{\max}$  are determined from a chunk of  $x$ .

## J. LLM Models

Parameters for some major transformer models are listed in Table 7. OPT model variants are listed in Table 5.

For LLM models, we used LLaVa: liuhaotian/llava-v1.6-vicuna-7b. It has Vicuna-7B model for LLM and ViT based on CLIP for the vision encoder. The Vicuna is an instruction-tuned version of LLaMa-2, having 32 transformer layers. CLIP ViT has 24 transformer layers.

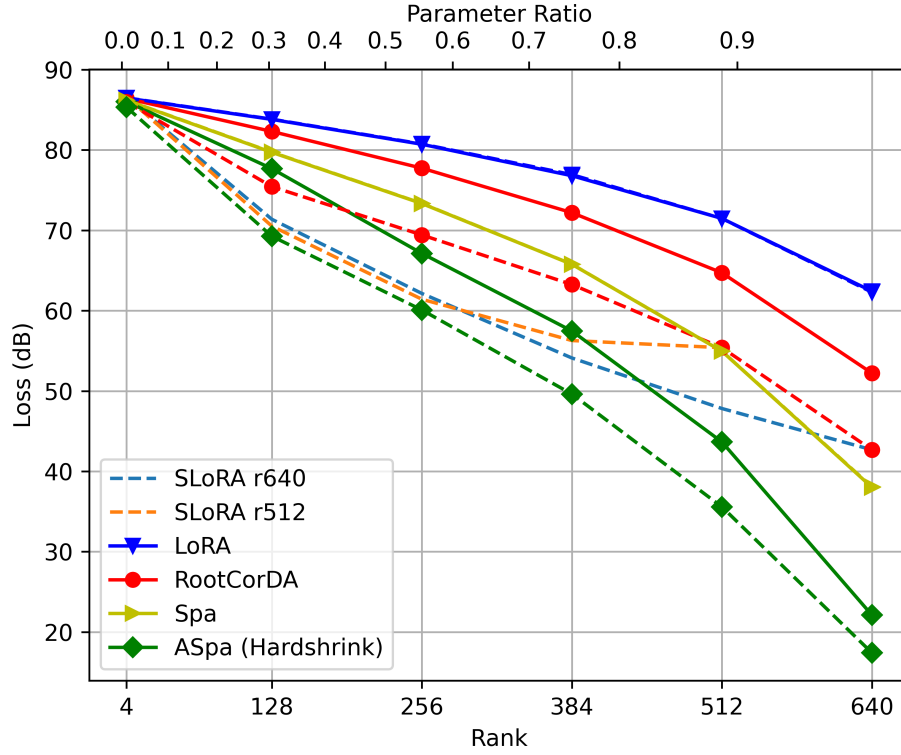


Figure 15. Sparsification of  $B$  and  $A$  low-rank matrices.

Table 5. OPT Models [49]

Models	# layers $L$	# heads $h$	hidden size $d$	head dim $d_h$	$d_i = 4d$	Huggingface ID
125M	12	12	768	64	3072	facebook/opt-125m
350M	24	16	1024	64	4096	facebook/opt-350m
1.3B	24	32	2048	64	8192	facebook/opt-1.3b
2.7B	32	32	2560	80	10240	facebook/opt-2.7b
6.7B	32	32	4096	128	16384	facebook/opt-6.7b
13B	40	40	5120	128	20480	facebook/opt-13b
30B	48	56	7168	128	28672	facebook/opt-30b
66B	64	72	9216	128	36864	facebook/opt-66b
175B	96	96	12288	128	49152	

Table 6. Qwen2 Models

Models	# layers $L$	# heads $h$	# KV heads $h_{kv}$	hidden size $d$	head dim $d_h$	$d_i$
0.5B	24	14	2	896	64	4864
1.5B	28	12	2	1536	128	8960
3B	36	16	2	2048	128	11008
7B	28	28	4	3584	128	18944
14B	40	40	4	5120	128	27392
32B	60	56	8	7168	128	28672
72B	32	32	32	4096	128	22016

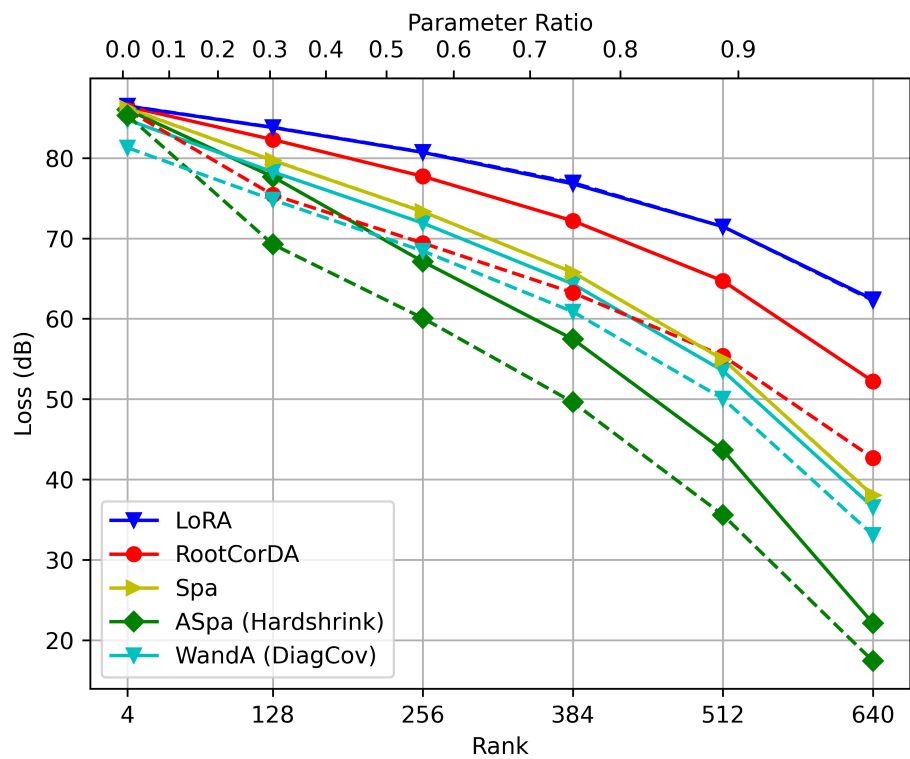


Figure 16. Comparison with WandA.

Table 7. Transformer Models

	ViT-16/B	Llama-2-7B	Llama-3.2-1B
ID	google/vit-base-patch16-224	meta-llama/Llama-2-7b-hf	meta-llama/Llama-3.2-1B-Instruct
hidden size $d$	768	4096	2048
hidden act	gelu	silu	silu
intermediate size $d_i$	3072 ( $4d$ )	11008 ( $2.68d$ )	8192 ( $4d$ )
head dim $d_h = d/h$	64	128	64
num attention heads $h$	12	32	32
num key value heads $h_{kv}$	12	32	8
num hidden layers $L$	12	32	16
qkv bias	True	False	False
mlp bias	True	False	False
rope theta $\theta$	—	1e4	5e5
max position embeddings	197	4096	131072
	OPT-350M	BLOOM-560M	Qwen2-0.5B
ID	facebook/opt-350m	bigscience/bloom-560m	Qwen/Qwen2-0.5B
hidden size	1024	1024	896
hidden act	relu	gelu	silu
intermediate size	4096	4096	4864
head dim	64	64	64
num attention heads	16	16	14
num key value heads	16	16	2
num hidden layers	24	24	24
qkv bias	True	True	True
mlp bias	True	True	False
rope theta	—	—	1e6
max position embeddings	2048	2048	131072
	RoBERTa-350M	Phi-3.5 mini	Gemma-2B
ID	FacebookAI/roberta-base	microsoft/Phi-3.5-mini-instruct	google/gemma-2b
hidden size	768	3072	2048
hidden act	gelu	silu	gelu
intermediate size	3072 ( $4d$ )	8192	16384
head dim	64	96	256
num attention heads	12	32	8
num key value heads	12	32	1
num hidden layers	12	32	18
qkv bias	True	False	False
mlp bias	True	False	False
rope theta	—	1e4	1e4
max position embeddings	514	131072	8192